African University of Science and Technology
Petroleum Engineering Stream, Abuja

THE STUDY OF HYDRODYNAMICS OF SLUG FLOW IN 10 DEGREES INCLINED PIPE USING ELECTRICAL CAPACITANCE TOMOGRAPHY DATA

A

THESIS

Presented to the Department of Petroleum Engineering,
The African University of Science and Technology,
[Abuja]

In Partial Fulfillment of the Requirements
For the Award of

MASTER OF SCIENCE

By
NWACHUKWU, CHRIS CHIAGOZIE

Abuja, Nigeria

November, 2014

THE STUDY OF HYDRODYNAMICS OF SLUG FLOW IN 10 DEGREES INCLINED PIPE USING ELECTRICAL CAPACITANCE TOMOGRAPHY DATA

By

Nwachukwu, Chris Chiagozie

A THESIS APPROVED BY THE PETROLEUM ENGINEERING DEPARTMENT

RECOMMENDED: …….

Supervisor, Dr. Mukhtar Abdulkadir

……

Committee Member

……

Committee Member

…….

Head, Department of Petroleum Engineering

APPROVED BY: ……..

Chief Academic Officer

.....

Date

ABSTRACT

Slug flow along slightly inclined horizontal pipes is a major problem in gas-liquid transportation, it is very pronounced in chemical, oil and gas processing industries. In reality, there is no absolute horizontal pipe due to the undulating nature/ Topography of the laid pipe terrains. Very little research has been done in this area because of lack of experimental data. This work is proposed to use raw experimental data from 10 degrees inclined horizontal pipe to analyze the flow properties and pattern. The experimental data obtained will be analyzed in order to improve the fundamental understanding of the flow regime promoted through them. The following parameters concerned with slug flow in a slightly inclined horizontal pipe: void fraction in the liquid slug, void fraction in the Taylor bubble, translational velocity, slug frequency, length of liquid slug and Taylor bubble will be determined using processed data obtained from Electrical Capacitance Tomography (ECT). The correlations from other studies such as Dukler et al(1975) ,Taitel et al (1990) etc will be used to validate the experimental results.

DEDICATION

To God almighty for his protection and provision: to the loving memory of my loving dad Late. Prof. P.A Nwachukwu, My mother Mr Alice. N Nwachukwu for her unfathomable love, patience and support to me in the pursuit of my studies; To my siblings: Chinenye and Obinna for their love and encouraging words during this endeavor; To my best friend, Miss Esther Kalu for her support during trial times. I want to specially dedicate this work to my top four financiers during this program Engr. Don Njoku, Barrister Mike Epelle, Mr Ikechukwu Ike, Mr Teddy Nwaokorie and Dr. (Mrs) Roseline Ugwuegbulam for their moral and financial support throughout my study period. May God replenish their pockets a million fold

ACKNOWLEDGEMENTS

First and foremost, I want to acknowledge God for blessing me with success and prosperity. I would like to thank all the people who have supported me in various ways throughout the period of this Msc research. In particular, I would like to thank my supervisors, Dr. Mukhtar Abdulkadir for his enthusiasm, guidance and continuous encouragement throughout the research. Special recognition is also paid to all my lecturers for their indelible impacts

I would like to take this golden opportunity to show my appreciation, gratitude and deep thanks to all those people who helped me during my stay in this university. I will like to acknowledge my two brothers with golden hearts: Ezzaka Otubo and Adum Lawrence for accommodating me throughout the program, I am still amazed by their generosity, may your cups never run dry. My stay in AUST was a miracle made flesh by human beings, to Sister Amarakristi Onyido for sacrificing all her dinner for me, to Monica Crankson for her love towards me even to her own detriments.to my very good friend Apisco you are more than an inspiration. I acknowledge all my class mates especially Lizzy , Sani Edwin, kizito, paulo and dauda to mention but a few

My thanks and gratitude also goes to some of the Phd students that touched my life in a special Mrs. Angela Nwachukwu, My mentor Mrs. Aborisade Opeyemi, Mr. Ignace Djitog, Mr Patrice Ndambomve, Mr. Mmaduabuchi Okpala, Mr. Yiporo Dayuo, Mr. Rwenyagila Egirudus and Mr. Emeka Ani. I absolutely could not have finished this program without their support, love and prayers.

Last but not least, I would like to extend my sincere gratitude to all the staff of AUST both academic and non-academic staff, you have always been there for me and there is no way I can repay you, my thesis dedication is the smallest gesture I can offer.

Contents

LIST OF TABLES

LIST OF FIGURES

CHAPTER ONE

INTRODUCTION

1.1 General introduction

Multiphase flows are of great interest to a large variety of industries. The power generation, nuclear reactor technology, food production, chemical process, petroleum, aerospace and automotive industries are all driving forces in this complex field. This work is concerned only with gas-liquid flows in inclined pipes with particular interest towards oil and gas industry applications.

1.1.1 Multiphase flow in pipes

The mixtures of two fluids in pipes are frequently encountered. Flow instabilities may cause the mixture to arrange itself into different geometric configurations. These geometric configurations are usually referred to as flow patterns or regimes. A little reflection will show that the orientation of the pipe makes a difference in the flow regime because of the role played by gravity and the density difference between the two fluids.

1.1.2 Flow patterns in gas-liquid pipe flow

When a gas-liquid mixture flows along a pipe, different flow patterns can be produced, influenced by several variables. Many flow patterns have been named in vertical, horizontal and inclined gas/liquid flow in pipes.

1.1.3 Flow patterns in horizontal systems.

Flow regimes in horizontal flow are illustrated in Figure 1.1. Here, as gravity acts perpendicular to flow direction, separation of the flow might occur. The respective flow regimes are stratified flow, where the gravitational separation is complete ;. stratified-wavy flow; bubble flow, where the bubbles are dispersed in the liquid continuum; annular dispersed flow, which is similar to that in vertical flow, though there is asymmetry in the film thickness due to the action of gravity; and a variety of intermittent flows. This latter category includes plug flow, in which there are large bubbles flowing near the top of the tube; semi-slug flow, where very large waves are present on the stratified layer; and slug flow, where these waves touch the top of the tube and form a liquid slug which passes rapidly along the channel.

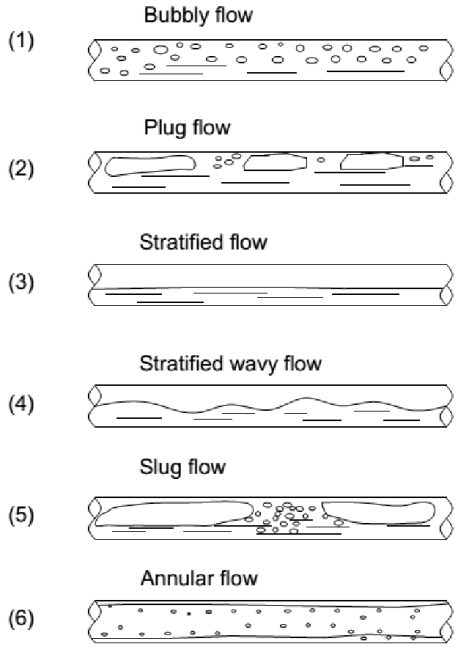

Figure 1.1:flow pattern in horizontal pipes

It is often necessary to predict regimes, and the usual procedure is to plot the information in terms of a flow regime map. Many of these maps are plotted in terms of primary variables (superficial velocity of the phases or mass flux and quality, for instance), but there has been a great deal of work aimed at generalizing the plots, so that they can be applied to a wide range of channel geometries and physical properties of the fluids.

1.1.4 Flow patterns in vertical systems.

The major flow patterns encountered in vertical co-current flow of gas and liquid (bubbly, slug, churn, and annular) are shown schematically in figure 1.2.

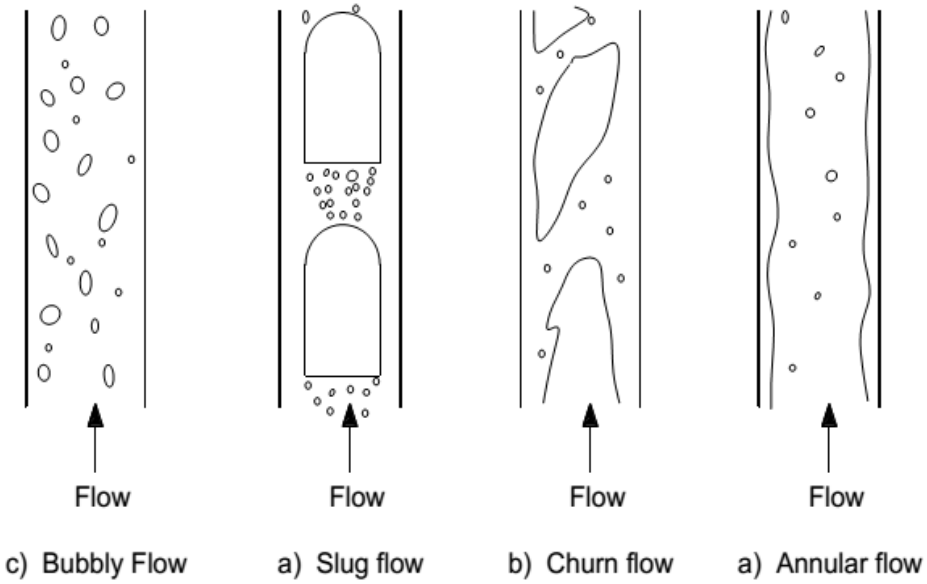

Figure 1.2: flow pattern in vertical pipes

At low gas flow rates, the gas phase tends to rise through the continuous liquid medium as small, discrete bubbles, giving rise to the name bubbly flow. As the gas flow rate increases, the smaller bubbles begin to coalesce and form larger bubbles. At sufficiently high gas flow

rates, the agglomerated bubbles become large enough to occupy almost the entire pipe cross section. These large bubbles, known as "Taylor bubbles," separate the liquid slugs between them. The liquid slugs, which usually contain smaller entrained gas bubbles, provide the name of the flow regime. At still higher flow rates, the shear stress between the Taylor bubble and the liquid film increases, finally causing a breakdown of the liquid film and the bubbles. The resultant churning motion of the fluids gives rise to the name of this flow pattern. The final flow pattern, annular flow, occurs at extremely high gas flow rates, which cause the entire gas phase to flow through the central portion of the tube. Some liquid is entrained in the gas core as droplets, while the rest of the liquid flows up the wall through the annulus formed by the tube wall and the gas core.

1.1.5 Flow patterns in upward inclined systems.

Flow patterns observed in upward inclined flow are quite similar to those observed in vertical upward flow, especially for near-vertical systems. They include bubbly and dispersed bubbly, slug, churn and annular flow in inclined systems, Figure 1.3.

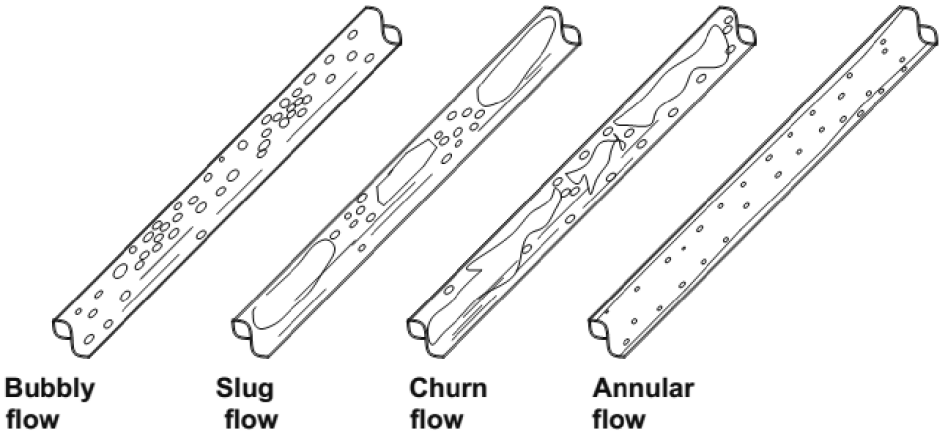

Figure 1.3: flow pattern in inclined pipes

1.2 Background to the research

This section gives a description of gas-liquid flow in horizontal pipe, the broad application of multiphase flow concept in different discipline and how the transition phases of the flow is characterized.

1.3 Problem statement

Several works have been done in describing flow regimes in horizontal pipelines and has resulted to so many correlations and models. However, in most of the work done they have been using fluids in small diameter pipes and whose density variation is almost minimal. However, this work is focused on using fluids with wide variation in terms of their viscosity (i.e. silicone oil and air), large diameter horizontal pipe and using modern techniques to observe the behavior of the fluids in 10 degrees inclined pipelines. Experimental investigation to study the behavior of gas-liquid mixture in a horizontal (10^o inclination) pipe was conducted by Abdulkadir, 2011 and data obtained will be analyzed in order to improve the fundamental understanding of the flow regime promoted through them. The following parameters concerned with slug flow in a 10 degrees inclined pipe: void fraction in the liquid slug, void fraction in the Taylor bubble, translational velocity, slug frequency, length of liquid slug and Taylor bubble will be determined using configuration using Electrical Capacitance Tomography (ECT) and some results will be compared to some empirical correlations obtained from literature.

1.4 Aim and objectives

The main **aim** and **objectives** of this work are:

1.4.1 Aim

To have a better understanding of the hydrodynamics of slug flow in a slightly inclined horizontal pipe.

1.4.2 Objectives

In order to achieve the aim of this study, the following objectives will be met:

(a) To process raw data obtained from an experimental investigation carried out by Abdulkadir (2011) on a horizontal pipe with an internal diameter of 67 mm, and 6 meter long to study air-silicone oil slug flow pattern in a horizontal orientation.

(b) To characterize slug flow, via the determination of the following: the translational velocity, void fraction in the liquid slug, void fraction in Taylor bubble, length of liquid slug and Taylor bubble, the frequency of slugging and the pressure drop.

(c) To validate some of the parameters highlighted in (b) with other correlations obtain from different studies and draw inferences.

1.5 Structure of the thesis

This work is divided into 5 chapters as described below and some other relevant information is provided in appendices:

Chapter 1 provides an introduction to the thesis, defining the problems, aims of the study and structure of the thesis.

Chapter 2 contains a review of published work on two-phase flows in pipelines. The flow patterns and flow pattern maps for the horizontal, vertical, and inclined pipes are described. Particular emphasis is given to models available for predict ing the liquid holdup, pressure drop, and slug characteristics

Chapter 3 describes the experimental apparatus; the properties of fluids used and the technique for measurements of liquid holdup and pressure drop. This chapter also includes a brief description of important facility components such as the data acquisition software and instrumentation.

Chapter 4 presents the experimental results obtained in the experiments per formed with a 67 mm pipe. The signal analysis that has been performed in order to process the data is explained together with the discussion of the data

Chapter 5 Brings together all the key conclusions from this work. Recommendations for further work are also provided.

CHAPTER TWO

LITERATURE REVIEW

In the literature, extensive studies exist on horizontal and vertically upwards gas liquid flow. These include models and correlations for flow pattern transitions, pressure drop and liquid holdup among other parameters. Commercial pipelines, however, follow normal terrain variations and consist almost entirely of uphill and downhill inclined sections, and therefore the models and correlations developed for horizontal or vertical flow are not always applicable, Hasan and Kabir (1988). Pipe inclination adds another dimension to the already complex flow phenomena, generally observed in horizontal and vertical pipes.

This chapter aims at highlighting the most relevant aspects related to the state of the art in the field on two-phase flow in inclined pipes. These are included in the following sections: 2.1 Flow pattern identification techniques, 2.2 Flow pattern maps, 2.3 Liquid holdup, 2.4 Pressure drop, 2.5 Slug flow characteristics and 2.6 Computational Fluid Dynamics.

2.1 Flow patterns in horizontal pipes

When two or more phases flow simultaneously in pipes, the flow behavior is much more complex than for single flow. The phases tend to separate because of differences in density. Shear stresses at the pipe wall are different for each phase as a result of their different densities and viscosities. Expansion of the highly compressible gas phase with decreasing pressure increases the in-situ volumetric flow rate of the gas. As a result, the gas and liquid phases

normally do not travel at the same velocity in the pipe. The flow patterns that exist during two or more phase fluid movement depend on the relative magnitude of the forces that act on the fluids. Buoyancy, turbulence, inertia and surface tension forces vary significantly with flow rates, pipe diameter, inclination angle and fluid properties of the phases.

Two phase flow patterns in horizontal tubes are similar to those in vertical flows but the distribution of the liquid is influenced by gravity that acts to ensure the liquid is confined at the bottom of the tube and the gas at the top. Flow patterns for co-current flow of gas and liquid in a horizontal pipe are characterized as follows:

- **Bubbly Flow**. The gas bubbles are dispersed in the liquid with a high concentration of bubbles in the upper half of the pipe due to their buoyancy. When shear forces are dominant, the bubbles tend to disperse uniformly in the pipe. In horizontal flows, the regime typically only occurs at high mass flow rates.
- **Stratified Flow.** At low liquid and gas velocities, complete separation of the two phases occurs. The gas goes to the top and the liquid to the bottom of the tube, separated by an undisturbed horizontal interface. Hence, the liquid and gas are fully stratified in this regime.
- **Stratified-Wavy Flow.** Further increasing the gas velocity, these interfacial waves become large enough to wash the top of the tube. This regime is characterized by large amplitude waves intermittently washing the top of the tube with smaller amplitude waves in between. Large amplitude waves often contain entrained bubbles. The top wall is nearly continuously wetted by the large amplitude waves and the thin liquid films left behind. Intermittent flow is also a composite of the plug and slug flow regimes. Those sub-categories are characterized as follows:

- ✓ **Plug Flow.** This flow regime has liquid plugs that are separated by elongated gas bubbles. The diameters of the elongated gas bubbles are smaller than the tube, such that, the liquid phase is continuous along the bottom of the tube below the elongated bubbles. Plug flow is also sometimes referred to as elongated bubble flow.
- ✓ **Slug Flow.** At higher gas velocities, the diameters of elongated bubbles become similar in size to the channel height. The liquid slug separating such elongated bubbles can also be described as large amplitude waves.

- **Annular Flow.** At even larger gas rates, the liquid forms a continuous annular film around the perimeter of the tube, similar to that in vertical flow but the liquid film is thicker at the bottom than the top. The interface between the liquid annulus and the vapour core is distributed by small amplitude waves and droplets may be dispersed in the gas core. At high gas fractions, the top of the tube with its thinner film becomes dry first, so that the annular film covers only part of the tube perimeter and thus this is then classified as stratified-wavy flow.
- **Mist Flow.** Similar to vertical flow, at very high gas velocities, all the liquid may be stripped from the wall and entrained as small droplets in the continuous gas phase (Engineering Data Book III, 2007).

2.2 Slug flow

The slug flow pattern is one of the most common flow patterns experienced during normal operating conditions of a two-phase pipeline. It is characterized by fast moving liquid slugs with high holdup values alternating with large gas pocket or film regions. The flow is very dynamic since the fast moving liquid slugs keep overriding slow moving liquid films in front of them. Thus a particle of liquid in the liquid film is continuously picked up by the front of the liquid slug, accelerated to a much faster velocity, then decelerated as it travels along the liquid slug body, and finally shed at the tail into the liquid film behind as the velocity approaches the film velocity once again. Hubbard (1965) and Dukler and Hubbard (1975) provided the first comprehensive slug flow model, which has served as a basis of slug flow modelling ever since.

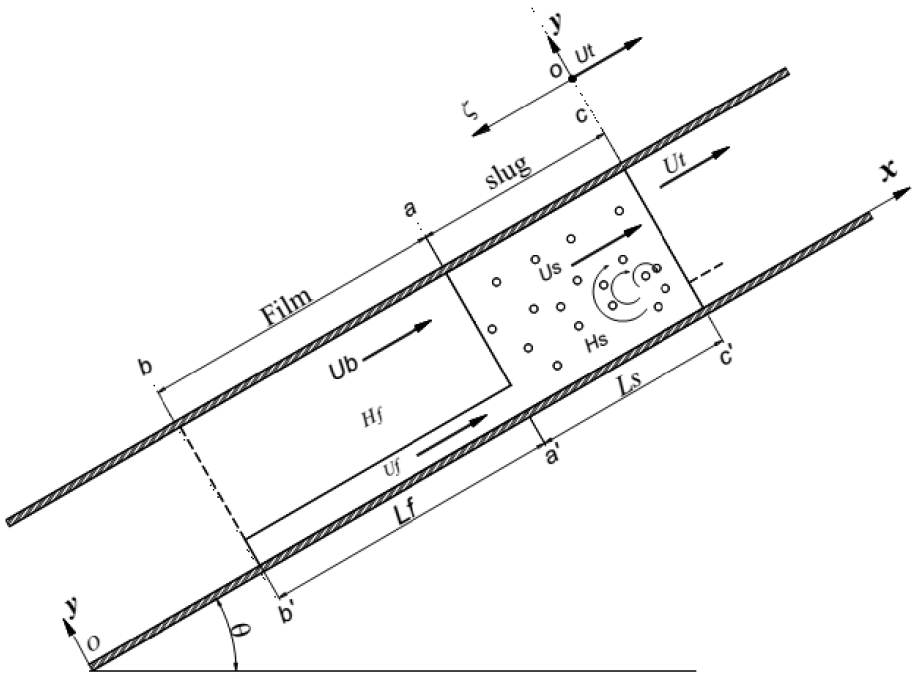

Figure 2.1:Slug Flow representation

Figure 2.1 shows a simplified physical model of slug flow. The model starts from the basic concept that a slug unit is composed of a slug body of length and liquid holdup L_S and H_S respectively, and a gas pocket and liquid film zone of length L_f with liquid holdup H_f respectively. At the front of the slug body, moving at the translational velocity U_t, there exist a mixing zone where liquid is scooped up from the film in front, and accelerated to the slug velocity, U_S. There are two velocity components associated with the film zone; U_f for the liquid film velocity, and U_{GP} for the gas pocket velocity. The model assumes that the amount of liquid scooped is equal to the amount of liquid shed; therefore, the length of the slug stays constant as it travels along the tube.

In order to develop the equations for the slug, the entire liquid film and the gas pocket in the film zone are used as the control volume, as shown in Figure 2.1. Continuity and momentum equations are derived for them relative to a coordinate system moving with the translational velocity U_t.

With the fully dispersed flow assumption, the unit cell representation leads to the idealized situation in which the flow is periodic both in time and space. Even if the flow is unsteady in the frame defined by the coordinate Ox, there exist a particular frame oζ moving with the cell at the velocity Ut so that the flow appears steady, the velocity of phase-k averaged over the pipe, Uk, is thus transformed by the change of frame as Ut -Uk.

2.2.1 Slug velocity

Dukler and Hubbard (1975) performed a liquid mass balance between the slug front and a point in the slug body with the fully accelerated slug velocity, US, which yields;

$$H_S(U_T - U_S) = H_F(U_T - U_T)$$

Equation (2.47) can be arranged in another form;

$$U_T = (1 + C)U_S \equiv C_O U_S$$

Where,

$$C = \frac{H_F}{H_S}\left(\frac{U_T - U_F}{U_S}\right)$$

It has been reported in the literature that C_0 varies between 1.2 and 1.35. Kouba (1987) experimentally concluded that C_0 can be as high as 1.8 for some flow conditions (low superficial liquid and gas velocities). More recently, Zheng et al.(1994) also reported an experimentally observed value of 1.20 for C_0 f or a wide range of slug flow conditions, even with inclination angles as high as 5˚. In most cases, C_0 only varies between 1.2 and 1.25. It is usually assumed a value of 1.2 for C_0, which would represent the maximum velocity for fully developed turbulent flow. In order to calculate the liquid slug velocity mass balances are performed for both phases between the inlet and any slug unit, and showed that;

$$U_S = U_M \equiv U_{SL} + U_{SG}$$

The slug is characterized by two interfacial velocities; the slug front and the bubble front. The bubble front translational velocity, V_{BF}, is often assumed to have the form as suggested by Nicholson *et. al* (1978).

$$V_{BF} = 1.2V_S + V_D$$

Where, Vs is the average velocity of the liquid in the slug. For homogeneous, no-slip flow in the slug body, Vs = Vm. Therefore, 1.2Vm is approximately equal to the maximum velocity of the liquid in the slug. The drift velocity, V_D, in Eq. 2.1 is then the relative velocity between the maximum gas velocity in the bubble, V_{BF}, and the maximum velocity of the liquid in the slug, 1.2Vs. While the drift velocity is clearly non-zero for inclined flow as reported by Hubbard and Dukler (1966); Gregory and Scott (1969); Heywood and Richardson (1979), reported that $V_D = 0$ for horizontal flow. Others like Kouba (1986); Nicholson *et. al*., (1978); Gregory and Mattar (1973), observed significant drift velocities in horizontal pipes. Weber explained why some investigators have not observed drift in horizontal pipes by performing a force balance on the nose of a stationary bubble. This revealed a critical Eotvos number below which liquid will not drain from a horizontal pipe opened to the atmosphere at one end and closed at the other, i.e. no drift. Weber (1981) also proposed the following correlation for the drift velocity in horizontal pipes:

$$\frac{V_D}{\sqrt{gd}} = 0.54 - 1.76\, {E_{oD}}^{-0.56}$$

Where

$$E_{oD} = \frac{\rho_L g d^2}{\sigma}$$

Bendiksen (1984) presented formula to calculate the bubble drift velocity in inclined pipes:

$$V_D = (V_D)_{horizontal}\, cos(\phi) + (V_D)_{vertical}\, sin(\phi)$$

Davies & Tayorli (1950) showed that, the bubble drift velocity in vertical tube is:

$$V_{D\,vertical} = 0.35\sqrt{gd}$$

For horizontal pipe, Benjamin (1968) proposed the following relation:

$$V_{D\,horizontal} = 0.54\sqrt{gd}$$

Equation 2.2 should be used in place of Equation 2.6 for cases when the Eotvos number is small (i.e. small diameter pipes or very viscous fluids). The slug front velocity can be obtained by performing a liquid mass balance between the slug front and a point in the slug body where it is assumed that the film has been fully accelerated to a velocity Vs:

$$V_{SF} = \frac{H_S V_S - H_f V_f}{H_S - H_f} = V_s + (V_s - V_t)\sum_{i=1}^{\infty}\left(\frac{H_f}{H_s}\right)^i$$

2.2.2 Slug holdup

The prediction of the liquid holdup in the slug body for two-phase gas-liquid slug flow is important for the accurate calculations of the pressure drop. Dukler and Hubbard (1975) showed that a void fraction in the slug depends on input gas liquid ratio. The effect of pipe has been investigated by Andreussi and Bendiksen (1989) and others. Fluid properties like surface tension and liquid density were included by Malnes (1983). A distinct dependency on pipe inclination was suggested by Andreussi et al. (1993). Brauner and Ullmann (2004) present a critical overview of the different approaches for modelling of the void fraction in slugs.A widely used correlation for estimation of gas fraction in slugs as a function of superficial mixture flow rate was presented by Gregory et al. (1978),

$$H_S = \frac{1}{1 + \left({}^{U_M}/_{8.66} \right)^{1.39}}$$

Where U_m is expressed in m/s. Gregory et al. (1978) cautioned that the use of this correlation should be limited to cases where U_m is less than 10 m/s to reduce the possibility of entering the transitional zone between slug and annular flows, where the correlation would not be applicable.

Malnes (1983) included fluid properties (surface tension and liquid density), and proposed the following correlation,

$$H_S = 1 - \frac{U_M}{\left[83 \left(\frac{g \sigma_{GL}}{\rho_L} \right)^{\frac{1}{4}} + U_M \right]}$$

Marcano et al. (1996) performed experiments in a d = 77.9 mm, L = 420 m horizontal pipeline. The fluids were kerosene and air, and the operational pressure approximately 5.5 bar. Based on void fraction measurements made by capacitance sensors, a correlation was proposed for void fraction in slugs,

$$H_S = \frac{1}{(1.001 + 0.0179U_M + 0.0011U_M)}$$

Where U_m is the mixture superficial velocity in [ft/s]

Gomez *et. al*. (2000) used data from a number of other authors with pressures from 1.5 to 20 bar, pipe diameters from 51 to 203 mm, and pipe inclination in the range of 0 - 90^o. The data indicated a clear dependency between pipe angles, slug Reynolds number (R_e), and slug void fraction. A correlation was suggested as equation (2.10).

$$H_s = e^{-(0.45\theta + CR_e)}, 0 \leq \theta_R \leq \frac{\pi}{2}$$

Where the pipe angle θ is in radian, the coefficient C= 2.48 $\times 10^{-6}$; slug Reynolds number is defined as: $Re_L = \frac{\rho_L v_m d}{\mu_L}$

Abdul-Majeed (2000) recently developed a new empirical equation for estimating the liquid slug holdup based on 316 data points for horizontal flow and 107 data points for slightly inclined flow. His analysis of the present studies, taken over a wide range of parameters, indicated that the slug holdup is only affected slightly by the pipe diameter and the surface tension, but is strongly influenced by the fluids dynamic viscosity. Therefore, he proposed the following correlation:

$$H_S = (1.009 - CU_M)A$$

Where the coefficient C is given by:

$$C = 0.006 + 1.3377 \frac{\mu_G}{\mu_L} \text{ ----------2.12}$$

The parameter A was included to account for the effect of pipe inclination and it is expressed as:

$$A = \begin{cases} 1 & if\ \beta \leq 0 \\ 1 - sin(\beta) & if\ \beta > 0 \end{cases} \text{ ---------- 2.13}$$

TABLE 2.1 Summary of slug body liquid holdup correlations to be considered in this work

MODEL	DIAMETER (mm)	FLUID	SLUG BODY HOLDUP
Gregory *et. al*. (1978)	25, 51	Air/Light Oil	$H_s = \frac{1}{1 + \left(\frac{U_m}{8.66}\right)^{1.39}}$
Marcano *et. al*. (1998)	78	Air/Kerosene	$H_s = \frac{1}{1.001 + 0.0179\,U_m + 0.0011 U_m^{\,2}}$
Gomez *et. al*. (2000)	51 to 203	Air/Water Air/Oil Freon/Water	$H_s = e^{-(0.45\theta + C R_e)}, 0 \le \theta_R \le \frac{\pi}{2}$ C= 2.48×10^{-6}; $Re_L = \frac{\rho_L U_m d}{\mu_L}$
Abdul-Majeed (2000)	25 to 203	Air/Water Air/Light Oil Air/Kerosene Freon/Water Nitrogen/ Diesel	$H_S = (1.009 - CU_M)A$ Where $C = 0.006 + 1.3377\,\frac{\mu_G}{\mu_L}$; $A = \begin{cases} 1 & if\ \beta \le 0 \\ 1 - sin(\beta) & if\ \beta > 0 \end{cases}$

2.2.3 Slug frequency

The frequency, f, is in fact defined as the mean number of slugs per unit time as seen by a fixed observer; Hubbard (1965), Gregory and Scott (1969). A very much used correlation for slug frequency prediction was developed by Gregory and Scott (1969) based on data by Hubbard (1965). Nydal (1991) compared the correlation with experimental data and found a good fit within the original data range (U_{SG}< 10 m/s and U_{SL}< 1.3 m/s).

$$f_S = 0.0226\left[\frac{U_{SL}}{gd}\left(\frac{19.75}{U_M}+U_M\right)\right]^{1.2}$$

A correlation was suggested by Greskovich and Shrier (1972). This model is on the same form as the Gregory and Scott correlation,

$$f_S = 0.0434\left[\lambda_L\left(\frac{2.02}{d}+\frac{{U_M}^2}{gd}\right)\right]^{1.02}$$

Tronconi (1990) presented a semi-mechanistic expression for the slug frequency, where the slug frequency was assumed to be half the frequency of unstable waves (slug precursors),

$$f_S = 0.305 Cw^{-1}\frac{\rho_G}{\rho_L}\frac{U_G}{h_g}$$

Where $U_G=U_{SG}/(1-H_L)$ h_G is the height of the gas phase at the inlet, immediately upstream the point of slug initiation. C_w is the wave velocity of the waves growing to become slugs. Tronconi postulated a linear relationship between the frequency of critical waves and the slug frequency, $f_w=C_w f_S$, with $C_w=2$.

This corresponds to observations in slug flow (by Dukler et al. (1985) and Kordyban(1985)), where every second slug originating from these waves was unstable and disappeared. The Tronconi correlation does not directly take into consideration any change in slug frequency with changing liquid flow rate, but indirectly through the calculations of gas flow rate and height.

Nydal (1991) argued that, at high liquid flow rates, the slug frequency should depend weakly on U_{SG}, but strongly on U_{SL}, and suggested a correlation based on the liquid flow rate alone,

$$f_S = 0.088\frac{(U_{SL} + 1.5)^2}{gd}$$

Jepson and Taylor (1993) published data from the 306 mm pipe diameter rig of the Harwell laboratory , and the effect of diameter was investigated by including 25 . and 51.2 mm pipe data from Nicholson et al. (1978). A non-dimensional slug frequency was correlated against the superficial mixture superficial velocity ,

$$f_S = \frac{U_{SL}}{gd}(7.59 \times 10^{-3}U_M + 0.01)$$

Manolis et al. (1995) developed a new correlation based on Gregory and Scott (1969). Taking $U_{m,min}$=5 m/s and the modified Froude number

$$fr_{mod} = \frac{U_{SL}}{gd}\left[\frac{{U_{M,min}}^2 + {U_m}^2}{U_m}\right]$$

Where

$$f_S = 0.0037 fr_{mod}^{1.8}$$

Zabaras (1999) suggested a modification to the Gregory and Scott correlation, where the influence of pipe inclination angle was included, equation (2.73). The data on which the modified correlation was tuned included positive pipe angles in the range of 0 to 11□ relative to the horizontal.

$$f_S = 0.0226 \left[\frac{U_{SL}}{gd}\left(\frac{19.75}{U_M} + U_M\right)\right]^{1.2} (0.836 + 2.75 \sin\theta)$$

TABLE 2.2 Summary of fully developed slug frequency models considered in this work

MODEL	DIAMETER (mm)	FLUID	SLUG FREQUENCY
Gregory & Scott (1969)	19	CO_2-Water	$V_s = 0.0226\left[\frac{U_{SL}}{gD}\left(\frac{19.75}{U_m}\right) + U_m\right]^{1.2}$
Greskovich and Shrier (1972)	45	CO_2-Water	$V_S = 0.0226\left[\frac{U_{SL}}{U_m}\left(\frac{2.02}{D} + \frac{{U_m}^2}{gD}\right)\right]^{1.2}$
Heywood and Richardson (1979)	42	Air/Water	$V_S = 0.0434\left[\frac{U_{SL}}{U_m}\left(\frac{2.02}{D} + \frac{{U_m}^2}{gD}\right)\right]^{1.02}$
Zabaras (1999)	25 to 203	Air/Water Air/Oil	$V_S = 0.0226\left[\frac{U_{SL}}{gD}\left(\frac{19.75}{U_m} + U_m\right)\right]^{1.2}(0.836 + 2.75Sin\,\theta)$
Nadal *et. al.* (1991)			$V_S = 0.088\,\frac{(U_{SL} + 1.5)^2}{gD}$

2.2.4 Mean Slug length

Slug length (or frequency) is required as an input parameter for virtually every slug flow model. The prediction of the slug length is perhaps the most difficult parameter that must be estimated. Slug length has been found to be strongly dependent on the diameter of the pipeline. This makes correlations obtained using small diameter test facilities difficult to scale-up to larger field scale facilities. For large diameter pipes, the correlations developed at the Prudhoe Bay field of Alaska have been the most successful. Scott *et. al.,* (1989) proposed a correlation for different pipe diameters.

$$Ln(L_s) = -25.41 + 28.50\left(\frac{LnD}{12}\right)^{0.1}$$

Although there is a strong correlation of slug length with pipeline diameter, at a particular diameter substantial variations in slug length are observed due to differing gas and liquid velocities.

According to Mandhane flow pattern map, results strongly indicate that slug lengths are the smallest when near the "center" of the slug flow pattern region on a flow pattern map. The largest slug lengths are observed near the transition boundaries to the other flow patterns.

Similar slug length behaviour has been reported for large diameter pipes, where larger slugs are reported at the slug flow transition boundaries and smaller slugs are observed as flow rates move further into the slug flow region. This indicates the difficulty encountered in attempting to correlate slug length. Some of the variation of slug length with flow rates can be explained through physical mechanisms. It is postulated that the lower left portion of the slug flow pattern is dominated by terrain effects and the pipeline system geometry. At the transition from stratified flow, a very few slugs exist in the pipeline. In this region there exit of a slug from the outlet of the pipeline is tightly coupled with the formation of a slug near the pipeline entrance. Thus the

distance between the pipeline outlet and the slug formation point partially dictates the resulting slug lengths. The large region in the center of the slug flow pattern exhibits the smallest slug lengths. Slugs in this region are relatively unaffected by small changes in pipeline inclination and principally controlled by the pipeline diameter. As the annular flow boundary is approached, slug lengths are again observed to increase. This principle is due to increased aeration of the slug, with liquid slug volumes remaining close to that observed near the center of the flow pattern. For much of the flow pattern, slug frequency is a function of the liquid superficial velocity alone. Slug length and frequency are related as follows:

$$V = \frac{L_S}{V_{SF}}$$

When slug frequency is used as input to a slug flow model, slug length becomes an indirect calculation. The value of slug length back calculated from Equation (2.15) is highly dependent on the accuracy of the bubble/film model used.

Based on field data obtained from the Prudhoe Bay oil field in Alaska, Brill *et. al*., (1981) included the effect of the pipe diameter and mixture superficial velocity in the mean slug length and proposed the following correlation:

$$Ln(L_S) = -3.851 + 0.059\,ln\left(\frac{V_m}{0.3048}\right) + 5.445\left[ln\left(\frac{D}{0.0254}\right)\right]^{0.5}$$

Norris (1982) modified the above expression using further data from the Prudhoe Bay field, and produced the following expression:

$$Ln(L_S) = -3.287 + 4.589\left[ln\left(\frac{D}{0.0254}\right)\right]^{0.5}$$

Scott *et. al*., (1986) attempted an improvement of the above correlation by accounting for two slug growth mechanisms, namely liquid pickup at the slug front and gas expansion within the slug body. They suggested that the mean slug length should be given by the following empirical equation:

$$Ln(L_s) = -26.6 + 28.495\left[ln\left(\frac{D}{0.0254}\right)\right]^{0.1}$$

CHAPTER THREE

EXPERIMENTATION

3.1 Introduction

The analyses performed on experimental laboratory data provide the main source of information about specific multiphase flow regimes. This chapter presents a detailed description of the experimental rig used to study the flow behavior present in horizontal orientated pipe and an overview of the experimental facility.

3.2 Overview of the experimental facility

The first series of experiments were performed on an inclinable pipe flow rig, shown in Figure 3.1. This rig had previously been employed in multiphase annular flow studies executed by Azzopardi *et. al*., (1997); Geraci *et. al.,* (2007a); Geraci *et. al*., (2007b) and more recently for the study of bubbly, slug and churn flow by Hernandez-Perez (2006), gas-liquid flow in 90^o bends by Abdulkadir (2011). The experimental facility consists of a main pipe flow test section made from transparent acrylic pipes of 0.067 m inside diameter and 6 m long to allow for the development of the injected flow over the length of the test section. The test section is constructed from a series of conjoined short sections of pipe with a flange joint at either end. Each of these smaller test sections may be easily installed or replaced, to lengthen or shorten the length of the test section. The rigid steel frame supporting the test pipe section is constructed to enable the test pipe section to be inclined at angles of from -5^o to 90^o to the horizontal. In this work, the pipe was made horizontal (0^o). The experimental rig was charged with an air/silicone oil mixture. The experiment was performed by Mukhtar Abdulkadir at an ambient laboratory temperature of approximately 20^oC. The physical properties of the fluids used in the experiments are as shown on Table 3.1.

Figure 3.1: Picture of the experimental rig. (Abdulkadir, 2011)

Table 3.1: Properties of the fluids at 1 bar and at the operating temperature of 20^{o}C

FLUID	DENSITY (Kgm^{-3})	VISCOSITY ($Kgm^{-1}s^{-1}$)	SURFACE TENSION (Nm^{-1})	THERMAL CONDUCTIVITY ($Wm^{-1}K^{-1}$)
Air	1.18	0.000018	0.02	0.1
Silicone Oil	900	0.00525		
Eotvos Number	Eo= 1981.67			
Dimensionless Inverse Viscosity	N_f = 9311.72			
Morton's Number	Mo = 1.035 X 0^{-6}			

(Abdulkadir, 2011)

3.3 Description of flow facility

The description of the flow facility was obtained from Abdulkadir (2011). The flow facility consists of a liquid storage tank, liquid centrifugal pump, compressed air line, liquid and air rotameters, and a cyclone (separator). The Beggs and Brill correlation (1973) was used to determine the pressure drop along the horizontal pipe flow test section. The silicone oil enters the mixing chamber. This ensures that the gas and liquid were well mixed at the entry region of the test pipe flow section. The inlet volumetric flow rates of the liquid and the air are determined by the use of rotameters mounted in line with the air and silicone oil pipe lines to the mixing chamber. The fluid inflow conditions for which experiments were carried out for the horizontal pipe is over a liquid superficial velocity range of 0.05 – 0.38 $ms^{-1}$and a gas superficial velocity of

range 0.34 – 0.95 ms^{-1}. Across this range of gas-liquid injections slug flow pattern could be observed using the experimental rig. Air was supplied to the mixing chamber from the laboratory compressed air rig main system at 3.2 barg through a control valve. It was fed into the facility through a 22 mm internal diameter stainless steel pipe. Both the air flow rate and gauge pressure were measured prior to entering the mixing section using a set of two air flow rotameters mounted in parallel that covered a wide range of flow rates as well as a pressure gauge meter, respectively. An air distributor is installed whose function is to make sure that all of the air coming into the pipe are well mixed and equally distributed across the cross section of the pipe (Abdulkadir, 2011).

"The silicone oil is stored in a liquid storage tank and was pumped into the mixing section using a centrifugal pump. A bypass valve maintains the circulation of the liquid flow. In addition, two liquid rotameters mounted in parallel were installed to measure the flow rates of the silicone oil entering the test pipe flow section. The liquid flow rate is controlled by valves. The two separate phases are then mixed within the gas-liquid mixing section. From the mixer, two phase mixture flows along the test pipe flow section before it reaches the measurement sections where the ECT is located. The ECT sensor is located at distances of 4.4 m from the mixer entry section at the base of the test pipe flow section. The two ECT measurement planes are separated by a distance of 89 mm and placed around the circumference of the pipe. The capacitance measurements provide a pair of time series of liquid holdup. The use of two such circumferential rings of sensor electrodes, located at a specified distance apart (also, known as twin-plane sensors), enables the determination of the velocity of periodic structures such as Taylor bubbles and liquid slugs. As the air-silicone oil mixture exits the test pipe flow section it is fed through a cyclone separator. The air is released to atmosphere from the top of the separator and the liquid drains to the bottom

under the influence of gravity and flows back to the main liquid storage tank" (Abdulkadir, 2011).

3.4 Flow facility components

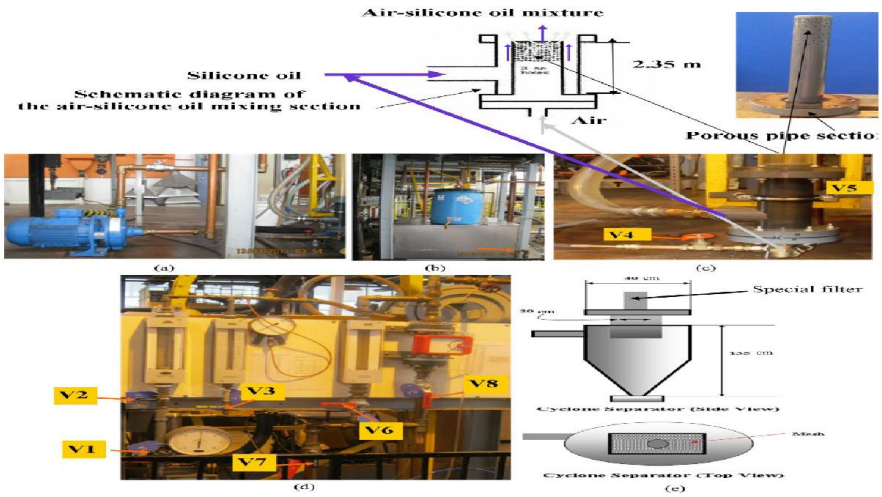

(Abdulkadir, 2011)

Figure 3.2: The major components of the rig, (a) Liquid Pump, (b) Liquid Tank, (c) Air-silicone Oil mixing section, (d) Rotameters, (e) Cyclone Separator

3.4.1 Gas-liquid mixing section

A number of different mixers for two-phase flow have been described by other investigators. The choice of mixer geometry is often dictated by the flow pattern that is of primary interest. For an investigation that covers the whole spectrum of flow patterns, Govier *et. al*., (1957) determined that the geometry of the mixing section affected the flow pattern only for a very short distance and that with an adequate calming section a simple "tee" was suitable (Abdulkadir, 2011).

"It was intended that the mixing of the air and silicone oil phases took place in such a way as to reduce flow instability. Flow stability was achieved by using a purpose built mixing unit,

providing maximum time for the two-phases to develop. The mixing section is made from PVC pipe as shown in Figure 3.2 c. The silicone oil was introduced from one side of the mixer. Air is fed from the rear of the mixing section directly through a distributor with 100 holes with a diameter of 3 mm each on the wall of the capped central pipe, thus creating a more even circumferential mixing section" (Abdulkadir, 2011).

.

3.4.2 Gas-liquid separation cyclone

"In the cyclone, the gas and liquid are separated by a combination of gravity and centrifugal effects. The centrifugal force throws the aerated liquid onto the vessel walls whereby it drains under gravity as a film. The diameter of the separator is 23.5 cm and height 1.35 m. The two-phase mixture is fed into the top of the cyclone tangentially. The separated air stream exits the top of the cyclone and the silicone oil returns by gravity feed through the bottom of the cyclone to the silicone oil reservoir tank (Figure 3.2 e)" (Abdulkadir, 2011).

3.4.3 Flow measurement section

The sections of flow measurement for both air and silicone oil are similar. The flow meter element was a rotameter of the type (Variable Area Meter). The two air rotameters together cover the range 10-1000 $Lmin^{-1}$. A picture of the flow measurement section is presented in Figure 3.2 d (Abdulkadir, 2011).

3.5 Pressure drop calculation

The total pressure drop calculations along horizontal pipe across a slug unit consist of two components: the accelerational pressure drop in the mixing zone and the frictional pressure drop in the slug body. For gas-liquid two-phase flow in horizontal pipes, the main contributor to pressure drop is the frictional shear stress between the slug body and the pipe wall; Whilst accelerational and gravitational body forces are negligibly small.

In this work, the modified Beggs and Brill correlation stated below is used to calculate the pressure drop along the entire 6 meters pipe using experimental variables.

The general pressure drop equation is given as:

$$-\frac{dP}{dz} = \frac{g\sin\theta}{g_c}\left(\rho_L H_L + \rho_G(1-H_L)\right) + \frac{f_m U_m^2 \rho_m}{2 g_c d} + \frac{f_m U_m}{g_c}\frac{dU_m}{dz} \quad \text{---------- 3.1}$$

Where g_c is a conversion factor to oil field unit.

Whilst the new definition of the two-phase friction factor by Beggs and Brill (1957) is given by the following expression:

$$\frac{1}{\sqrt{f_m}} = -2\log\left[\frac{1}{3.7065}\frac{\varepsilon}{d} - \frac{5.0452}{Re_m}\log\left(\frac{1}{2.8257}\left(\frac{\varepsilon}{d}\right)^{1.1098} \frac{5.8506}{(Re_m)^{0.8981}}\right)\right] \quad \text{---------- 3.2}$$

Where "ε" is the surface roughness and mixture Reynold's number (Re_m) can be calculated using the following relation:

$$Re_m = \frac{\rho_m U_m D}{\mu_m} \quad \text{---------- 3.3}$$

As mostly stated in literature, mixture density and mixture viscosity are:

$$\rho_m = \rho_L H_L + (1-H_L)\rho_g \quad \text{---------- 3.4}$$

$$\mu_m = \mu_L H_L + (1 - H_L)\mu_g \text{----------} \quad (3.5)$$

After the calculation of the necessary parameters, the gravitational, frictional and accelerational pressure drops are calculated from which representative results in the form of graphs are drawn as seen in chapter four.

3.6 Determination of the characterization parameters

3.6.1 Translational velocity of a Taylor bubble

Cross-correlation of the holdup time series produced by the two ECT planes located at 4.4 and 4.489 m above the mixer section at the base of the riser allow the time for the individual slugs to travel between the two planes to be determined. With the knowledge of time and the distance between the two planes (0.089 m), the translational velocity of periodical structures such as slugs can be calculated. The cross-correlation operation gives the linear dependence between the two time series data sets, x and y. Details can be found in Abdulkadir (2011) and Bendat and Piersol (1980). In this work, the set of equations for cross-correlation were programmed as a computational MACRO program to determine the translational velocity of the Taylor bubble and liquid slug.

3.6.2 Liquid film thickness

In this work, the film thickness was determined by the expression proposed by Fernandes *et al*. (1983)

$$\delta = \frac{D}{2}(1-\sqrt{\varepsilon_{TB}}) \text{ ---------- } 3.6$$

Where δ the film thickness in mm, D is internal pipe diameter in mm and ε_{TB} is the experimental measured void fraction in the Taylor bubble.

3.6.3 Slug frequency

In this work, the frequency of slugs was determined by two methods: (1) using the methodology of Power Spectral Density (PSD) as defined by Bendat and Piersol (1980). The PSD function was programmed as a computational MACRO program to determine the slug frequency. (2) The second methodology involved manual counting; counting the number of slugs present in a selected interval of time in a given time series of void fraction.

3.6.4 Lengths of the slug unit, the Taylor bubble and the liquid slug

The methodology for determining the stated lengths was the method adopted by Abdulkadir (2011). It is worth mentioning that a slug unit is defined as a Taylor bubble and the following liquid slug. In his work, the length of a slug unit was determined from the knowledge of the translational velocity of the Taylor bubble and the slug frequency that is, using equation (3.7)

$$L_{SU} = \frac{U_N}{f} \text{ ----------} 3.7$$

Where, f is the slug frequency and L_{SU} the length of slug unit

The length of individual Taylor bubble was determined as the difference between the lengths of slug unit and liquid slug. On the other hand, the length of individual liquid slug was determined from equation (3.8)

$$L_{Si} = \frac{L_{SUi}}{c+1} \quad \text{----------} \quad 3.8$$

Where L_{Si} is the length of individual liquid slug and c is a constant determined from the time series of void fraction

3.7 Schematic diagram of horizontal pipe

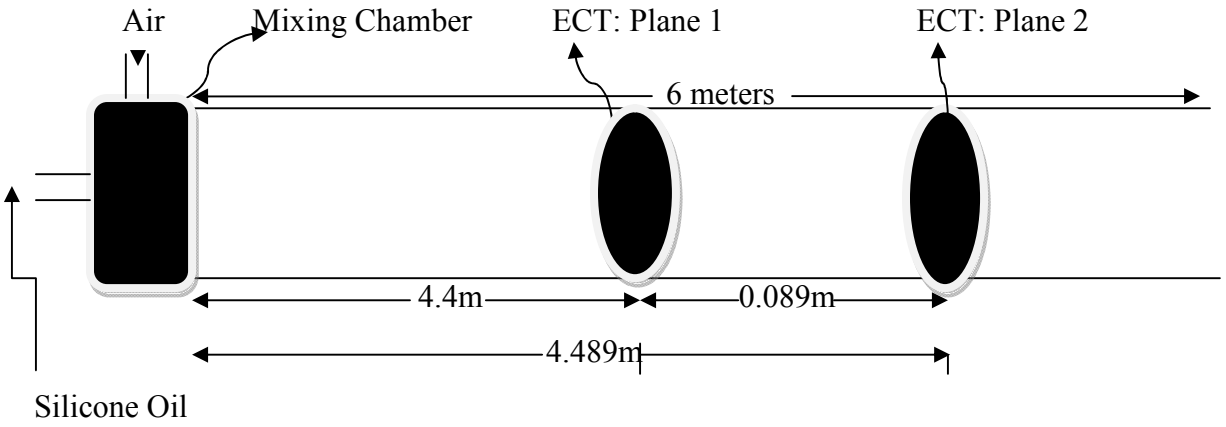

Figure 3.3: Schematic diagram of the horizontal 0^o inclination pipe

3.8 Electrical Capacitance Tomography (ECT)

The basic idea of the ECT is to install a number of sensors around the external circumference of the pipe to be imaged. The sensor output signals depend on the position of the component boundaries within their sensing zones. A computer is used to construct a tomographic image of the cross-section being observed by the sensors. This will provide for instance, measurements of two-phase flow boundaries in pipes with applications to multiphase flow measurements.

According to Bolton *et. al*., (1998), the objective of ECT is to provide images of phase distribution by exploiting differences in electrical permittivity between the phases of a multiphase flow mixture within a process vessel or pipeline. To facilitate measurements throughout the sensing zone, multiple electrodes are arranged around the boundary of the zone. The capacitance electrodes are usually made from thin copper films, and are attached to the outside of an insulated section of the process vessel or pipeline, resulting in electrodes that are truly non-invasive and non-intrusive. Typically, the sensor consists of 8 or 12 electrodes mounted symmetrically around the sensing zone (Wang *et. al.,* 1995 and Yang, 1996). Capacitance measurements are taken between all independent pairs of electrodes. In this study, the number of sensor consists of 8 electrodes. An essential requirement of the imaging system is that the measuring circuit should only measure the capacitance between the selected pair of electrodes and that it should be insensitive to stray capacitance between the measuring electrodes and earth. Therefore, to satisfy these requirements a stray immune capacitance measuring circuit, which uses switched-capacitor charge transfer, is used, (Xie *et. al*., 1992). The electrical capacitance tomography (ECT) system used in this work is a PTL-300 system, supplied by Process Tomography Limited. It consists of a data processing unit PC, DAM-200 data acquisition unit and a capacitance sensor. The PC runs the ECT 32 program and the twin-plane ECT software designed for the PTL-300 system, and runs under the Windows XP operating system. The ECT 32 program allows one or two ECT sensor planes to be controlled either independently or simultaneously, the data are captured and can be played back at different frame rates. The measurement data can be displayed as permittivity images, normalised capacitances or a combination of both. The DAM-200 unit hosts the twelve-channel inlets for the single and twin-plane arrangements, and must be connected to the PC at all times. If communications

between the PC and the DAM-200 are interrupted, the PC will enter an indeterminate state and it will be necessary to reboot the system to resume operation (Abdulkadir, 2011).

For details on process of raw data acquisition, calibration, image reconstruction process, void fraction measurement, methodology during an experimental runs from ECT, hazard analysis of experimental facility, percentage error estimation of data accuracy, and uncertainty analysis of the experimental measurement, refer to Abdulkadir (2011).

Table 3.2 Uncertainty of the experimental measurements

MEASUREMENT	UNCERTAINTY (m/s)
Mixture superficial velocity	± 0.0563
Liquid superficial velocity	± 0.0473
Gas superficial velocity	± 0.0304

(Abdulkadir, 2011)

3.9 Experimental measurement used to obtain the parametric characterization of the slug flow regime

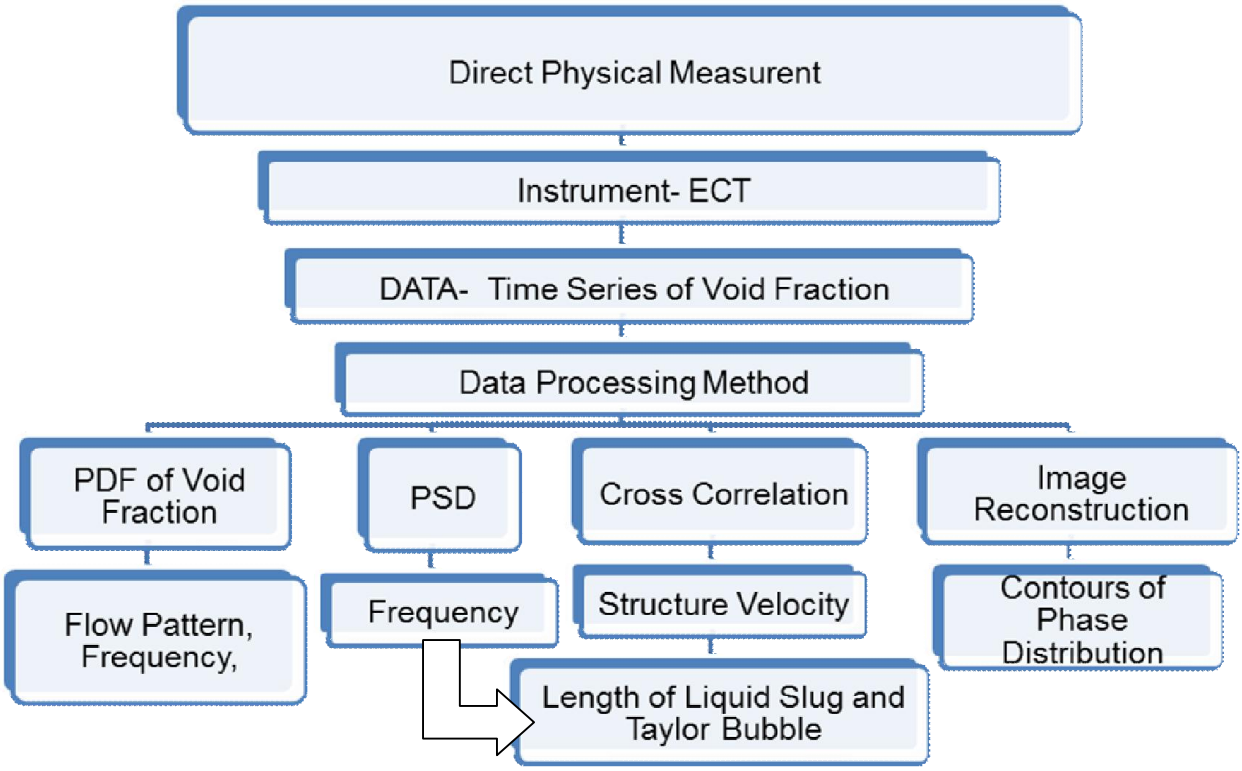

Figure 3.4-Experimental measurement used to obtain the parametric characterisation of the slug flow regime (Abdulkadir, 2011)

CHAPTER FOUR

RESULTS AND DISCUSSIONS

4.1 Introduction

In this chapter the results of the experiments carried out in a 67 mm pipe will be presented. The experimental arrangement was described in Chapter 3. The analysis is based on processed data derived from raw data output from a series of two-phase air-silicone oil flow laboratory experiments that were performed by Mukhtar Abdulkadir (2011) on a 10 degrees off the 10 degrees inclined pipe flow rig which is available within the L3 Laboratories of the Department of Chemical and Environmental Engineering at the University of Nottingham. . In the experiments performed, measurements of liquid holdup were taken at two locations downstream of the mixing section for horizontal and different inclinations for a wide range of flow rates.

4.2 Flow pattern in inclined pipe

The dominant flow pattern that is of great interest to this research is the slug flow. It is the purpose of this section to provide information about slug characteristics. In most cases, a successful recognition of slug flow has been obtained by monitoring the liquid phase fraction in the pipe with the ECT and plotting the PDF. Whenever the shape of the PDF presents a double peak, then slug flow has been identified as proposed by Khatib and Richardson (1984) and Costigan and Whalley (1997) .

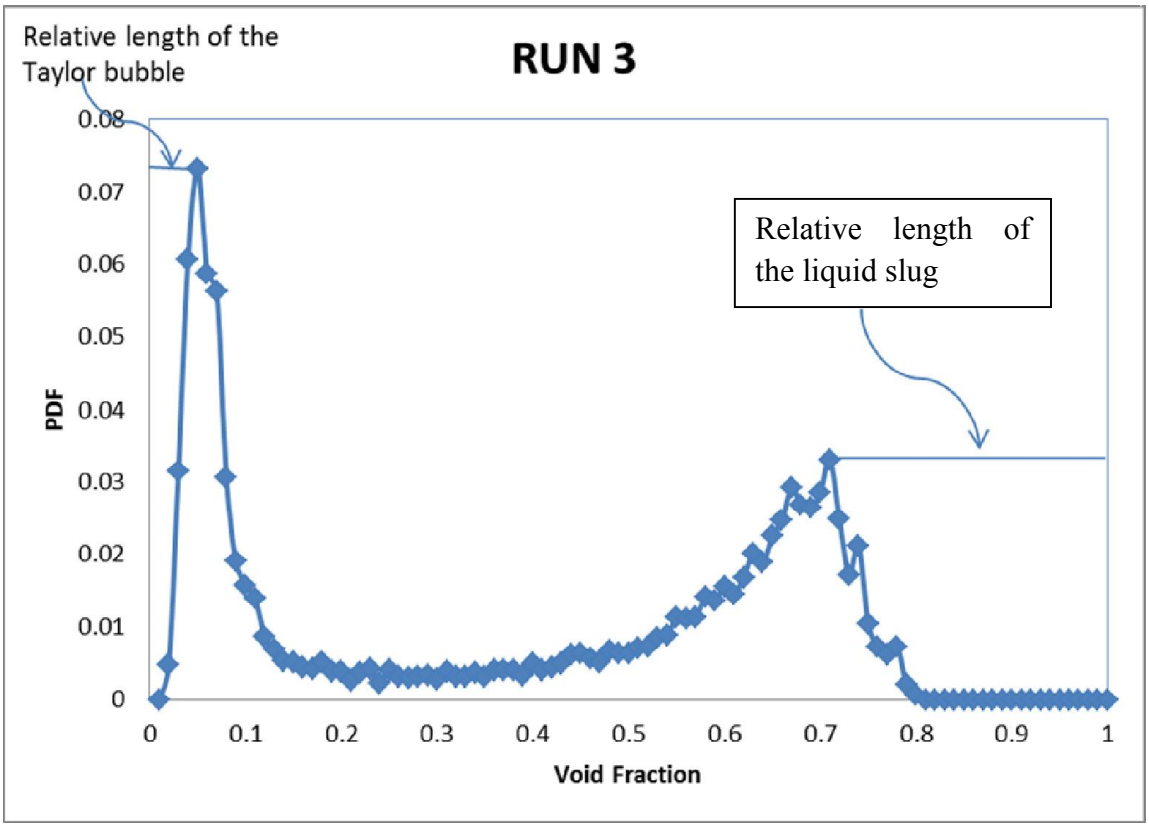

Figure 4.1: PDF of cross-sectional average void fraction for the case of slug flow measured from the experiments using air-silicone oil. The location of the peak in the low void fraction region represents the average void fraction in liquid slug, while its height represents the relative length of the liquid slug section.

4.3 Translational (Structure) velocity

Cross-correlation of the holdup time series produced by the two ECT devices allows the translational velocity of periodical structures such as slugs to be determined. A plot of time series for the two ECT devices is shown below in Figure 4.2.

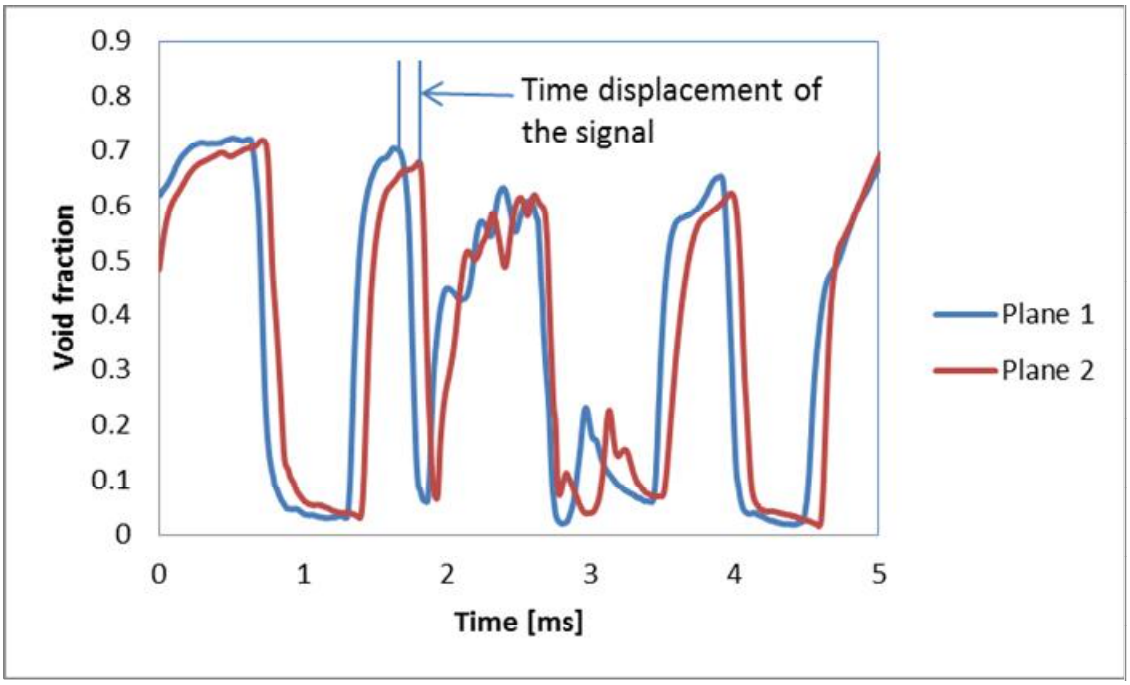

Figure 4.2 Liquid holdup signals from the two ECT devices;10 degrees inclination angle,

It is important to note that the drift velocity and translational velocity are affected by liquid velocity (Hernandez-Perez, 2007). Figure 4.3 shows a plot of the structure velocity as a function of mixture superficial velocity . As expected, a linear relationship is obtained between them. The drift velocity for the present studies can be taken as the Y-intersection of a line that fits the data points which is 0.6175 m/s, while the distribution coefficient is given by the slope of the line as 1.2078.

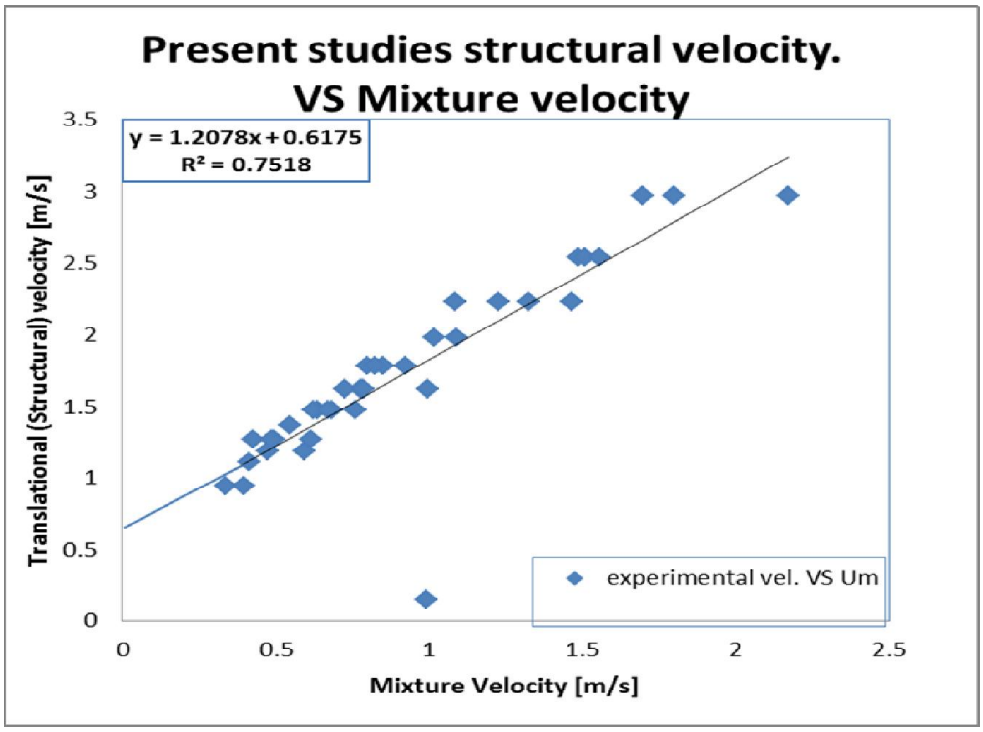

Figure 4.3: Experimentally measured translational (structure) velocity against mixture superficial velocity

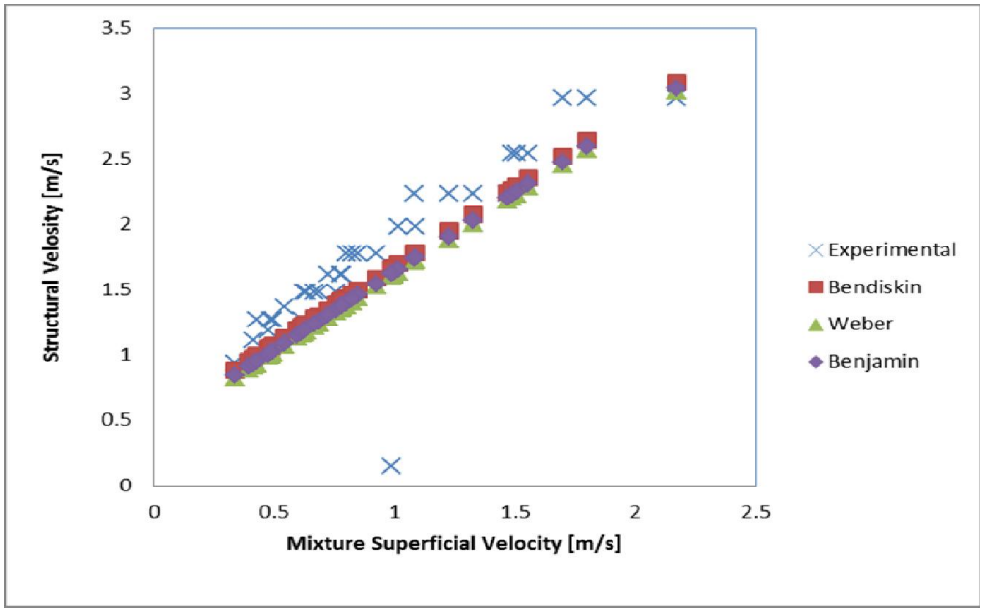

Figure 4.4: Experimentally measured translational (structure) velocity against mixture superficial velocity . The empirical equations proposed by Bendiksen (1984), Benjamin (1968) and Weber (1981) were recalculated using the physical properties of air and silicone oil.

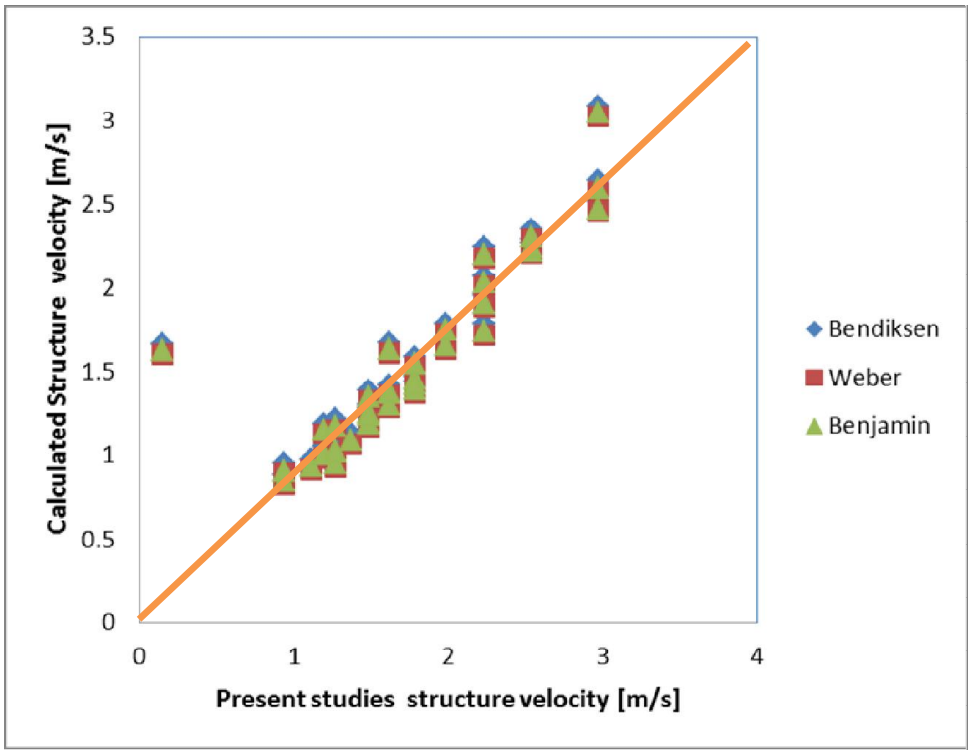

Figure 4.5: Comparison between experimentally measured translational (structure) velocity and empirically calculated structure velocity proposed by Bendiksen (1984), Benjamin (1968) and Weber (1981).

For the purpose of validating the result obtained from the present studies, the results were compared with correlations of Bendiksen (1984), Benjamin (1968) and Weber (1981) and are presented in Figures 4.4 and 4.5.

From figure 4.5, it can be observed that the Bendiksen (1984), Benjamin (1968) and Weber (1981) relations, with distribution coefficient of 1.2, slightly under predicted the Taylor bubble velocity over the range of flow conditions of the present work. From the present studies, the value obtained for the distribution coefficient is 1.21; however the experimental drift velocity of 0.6175 m/s is higher than the predicted drift velocities. For the predicted drift velocities, Bendiksen (1984), Benjamin (1968) and Weber (1981) obtained 0.438, 0.439 and 0.417 m/s

respectively. This can be attributed to the assumptions made by the respective researchers. Benjamin (1968) calculated the value of the drift velocity coefficient by using inviscid potential flow theory that inherently neglects surface tension and viscosity. Bendiksen (1984) showed that drift velocity is as a result of hydrostatic pressure difference between the top and bottom of the bubble nose. Weber (1981) developed his correlation for the drift velocity in horizontal pipe on the basis of experimental data of Zukoski (1966) for liquids of low viscosities.

4.4 Pressure drop

Pressure drop is an important parameter in pipeline design. The pressure drop in a system is an essential variable for the determination of the pumping energy for a given flow. The diversity of techniques used by different authors to present the two-phase flow pressure drop (Baker (1957), Griffith and Wallis (1961), Bonnecaze *et al.* (1971), Grescovich and Shrier (1971), Chen and Spedding (1981) and Jepson and Taylor (1993), indicates among other things, that pressure drop in two-phase flow can depend on a significant number of variables such as mass flow rate, which reduces with increasing void fraction; inclusion-induced wall shear, which increases with void-fraction where the conduit diameter is of no less importance.

The effect of gravity on the pressure drop is intuitive. Pressure drop is higher in the case of flow against gravity as compared to zero gravity and flow-along gravity cases in that order.

In this work, Beggs and Brill (1973) correlation as described in chapter three was used and results onbtained are presented in the Figures 4.6, 4.7, 4.8 and 4.9.

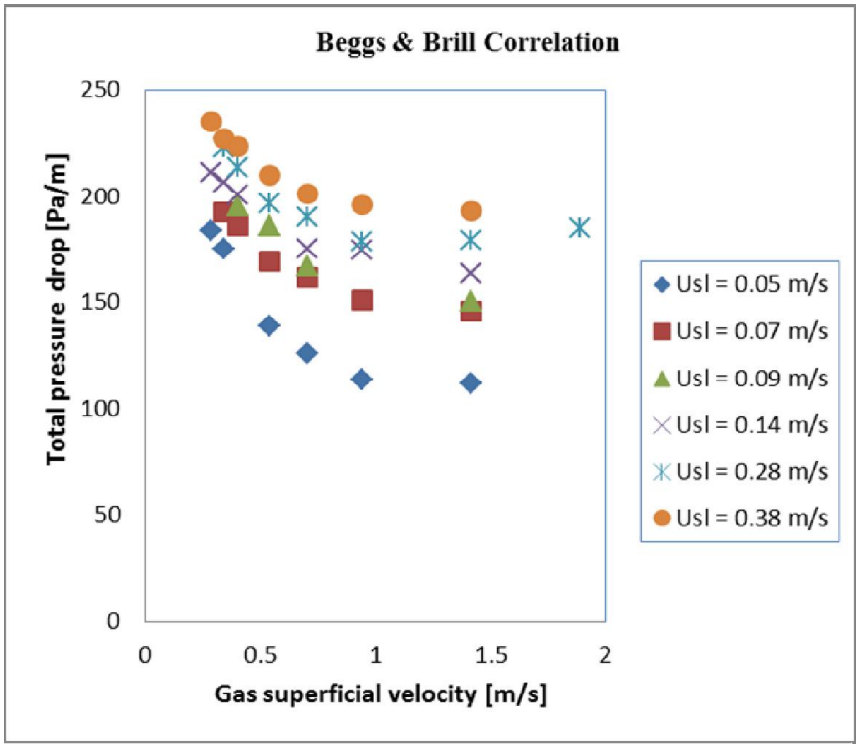

Figure 4.6: Influence of gas superficial velocities on the total pressure drop at varying liquid superficial velocities.

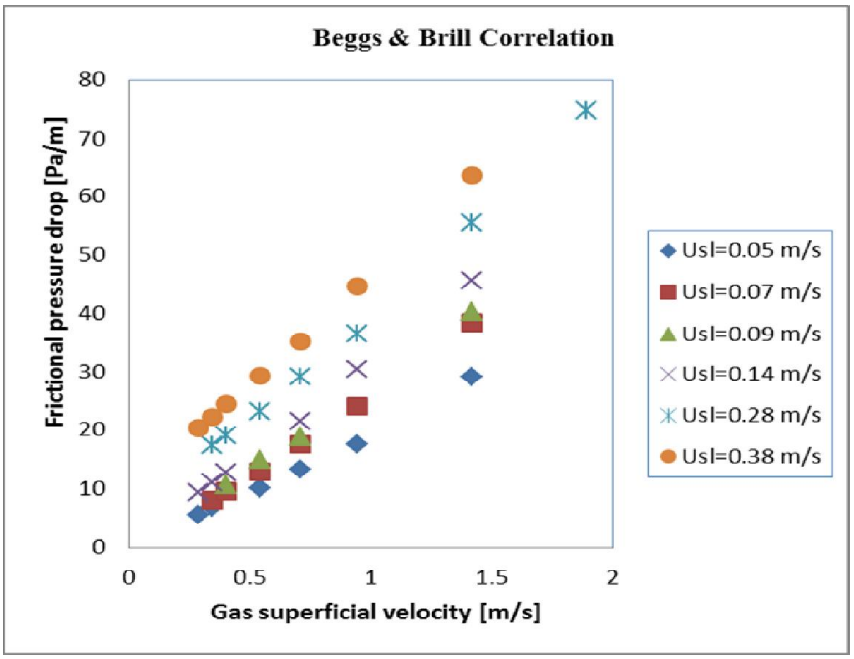

Figure 4.7: Influence of gas superficial velocities on the frictional pressure drop at varying liquid superficial velocities.

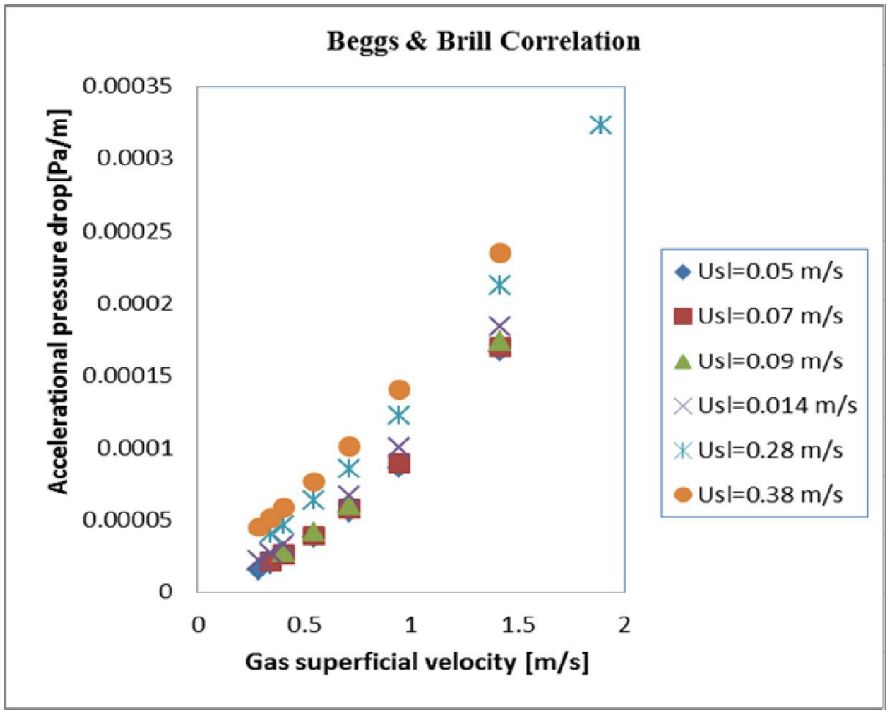

Figure 4.8: Influence of gas superficial velocities on the accelerational pressure drop at different liquid superficial velocities

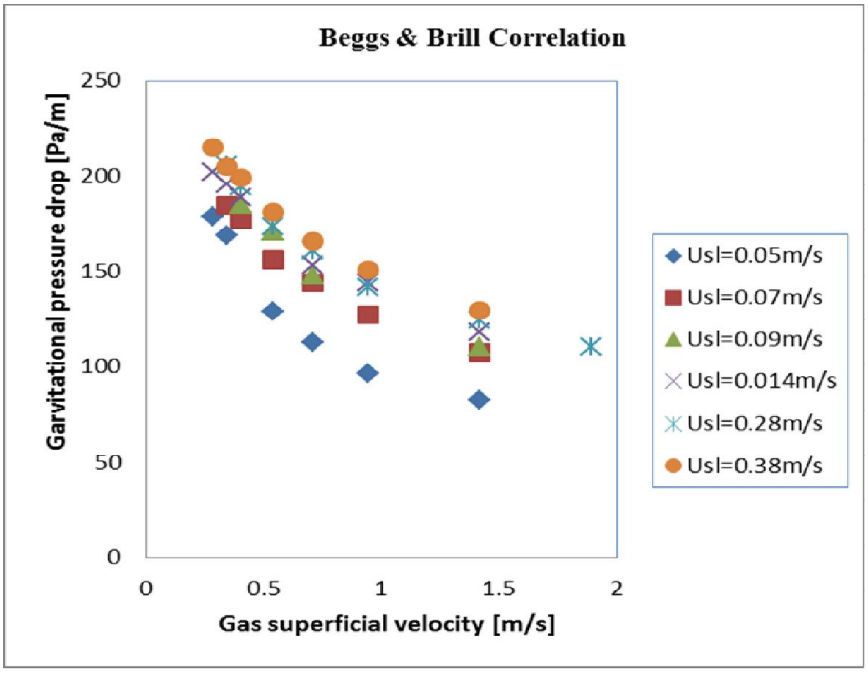

Figure 4.9: Influence of gas superficial velocities on the gravitational pressure drop at different liquid superficial velocities

Figures 4.6, 4.7, 4.8 and 4.9 clearly indicates that for flows in 10 degrees inclined pipes, the main contributor for the total pressure drop is the gravitational pressure drop, which is dependent on the pipe orientation, followed by frictional pressure drop which in turn is a function of the in-situ superficial velocity of the fluids. This fact is proved by the present studies in the above sited figures.

It is interesting to note that for a given liquid superficial velocity, the gravitational pressure drop decreases with increase in both gas superficial velocities. This decrease can be attributed to the fact that flow in 10 degrees inclined pipe is greatly affected by gravity due to the pipe inclination, whilst the accelerational pressure drop is negligibly very small but increases with increasing gas superficial velocity. This signifies that the lower the mixture density due to increasing gas superficial velocity, the higher the frictional pressure drop, hence, the higher the total pressure drop will be. Also, having a closer look at the variation of the frictional pressure drop with liquid superficial velocity, it was noticed that as the liquid superficial velocity increases, the frictional pressure drop also increases. This can be attributed to the increase in shear stress between the liquid and the walls of the tube and comparatively larger bubbles are observed to form due to coalescence, which causes a decrease in the liquid velocity due to higher level of liquid holdup, hence increases the frictional pressure drop. These observations support the phenomena reported by Beggs and Brill (1973) and Dukler and Hubbard (1975).

4.5 Void fraction in liquid slug

Void fraction in liquid slug is a very important parameter to be considered when characterizing slug flow in pipes 10 degree off the horizontal. The void fraction in the liquid slug described in the literature is related to the bubble entrainment, which is enhanced by the action gas superficial velocity and the interfacial shear stress. Knowledge of the bubble size is very important to characterize the internal structure of the liquid slug body. It can be concluded that as the gas superficial velocity increases, the bigger bubbles have major contribution to the void fraction in the liquid slug body.

The experimental result for the liquid slug holdup is shown in Figure 4.6.

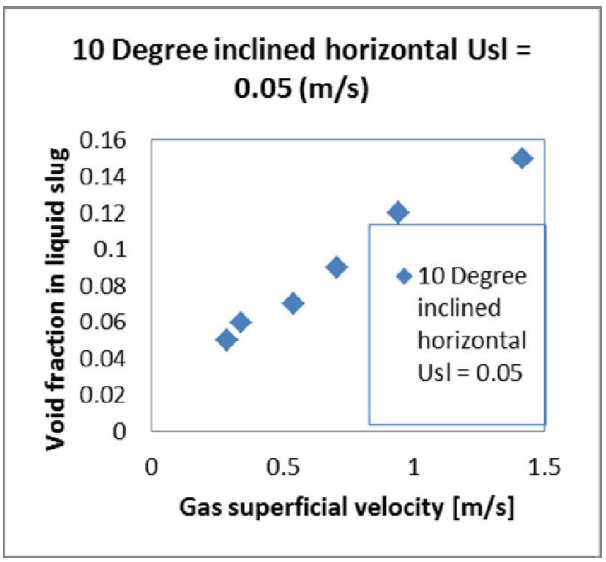

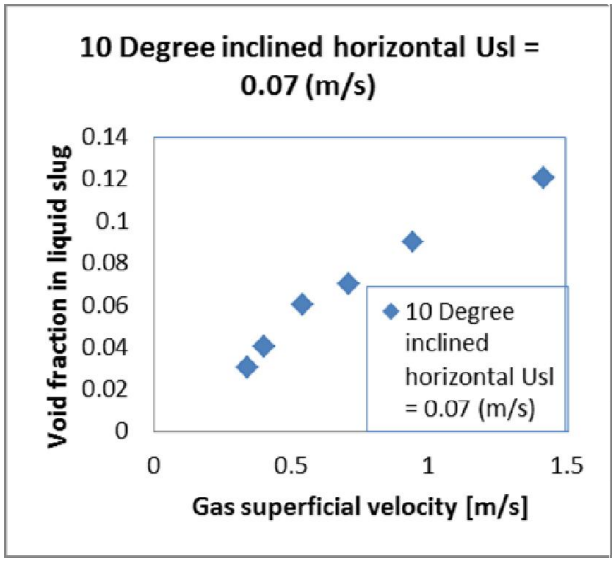

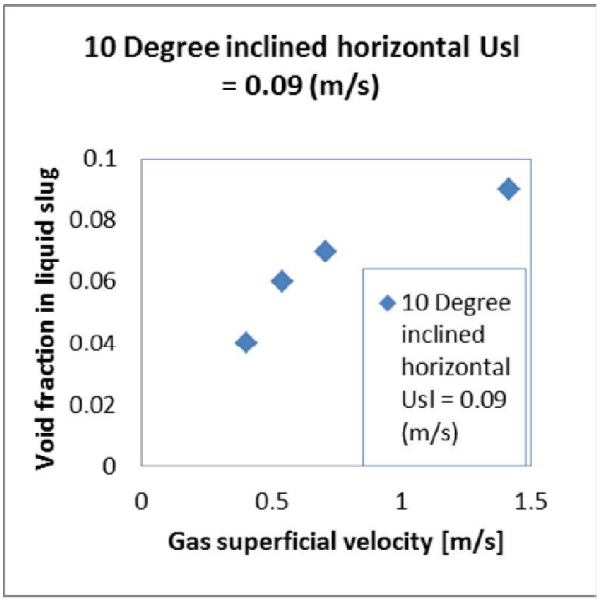

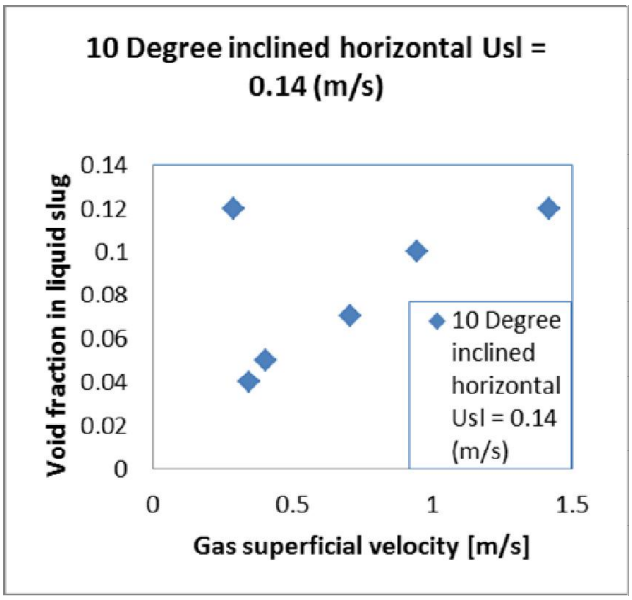

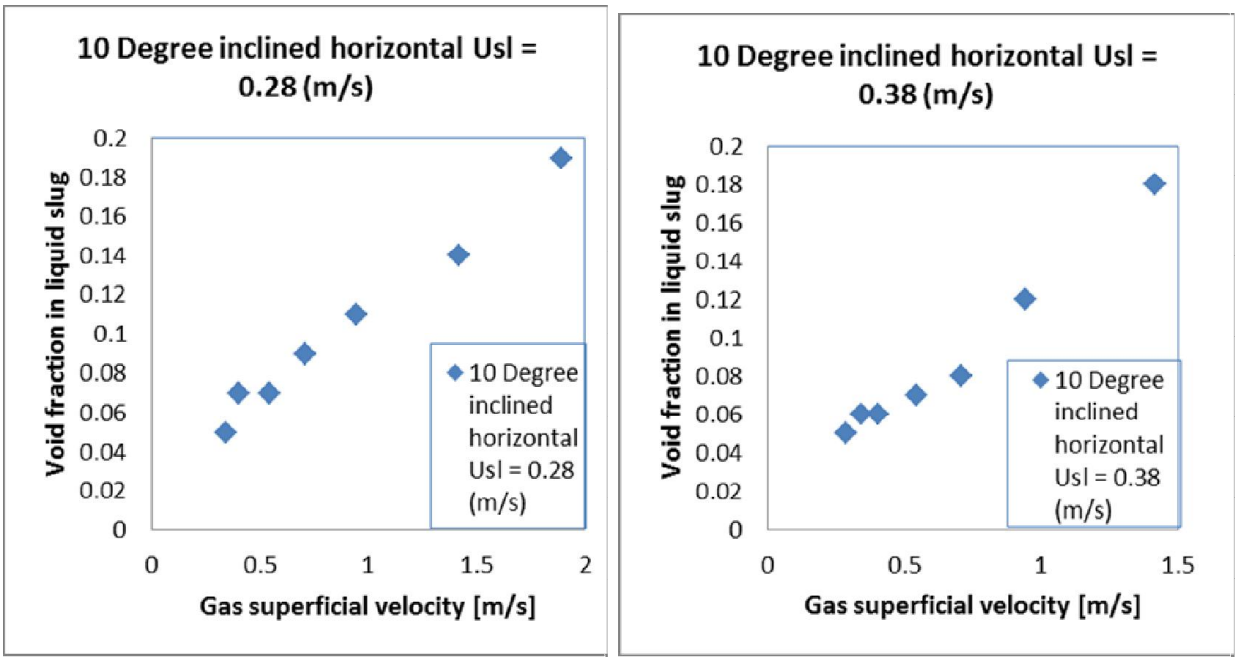

Figure 4.10: The determined void fraction in liquid slug at different liquid and gas superficial velocities

The void fraction measurements distinguish the large bubble contribution from those of the small bubbles present in the liquid slug. Thus the total void fraction is composed of these two contributions.

It is evident from Figure 4.6 that the void fraction shows a sharp increase practically getting close to one with increasing gas superficial velocity at constant liquid superficial velocity of 0.05 m/s. This is normally observed towards the top of the pipe, indicating the existence of a gas layer free of liquid at high gas superficial velocity. This is consistent with the observations made by de Chard and Delhaye (1996) that the void fraction in the liquid slug is zero.

As the air mass flux increases due to an increase in gas superficial velocity, the value of the void fraction tend to increase at the top part of the pipe with minimal change at the lower portion of

the pipe. This is observed when the liquid superficial velocity was kept constant at 0.09 m/s, the void fraction was almost uniform with increase gas superficial velocity and observed a sharp but gradual increase in the void fraction with further increase in superficial velocity. This sharp but gradual increase in the void fraction may be attributed to air entrainment of the liquid layer as a result of an increase in the gas flow rate.

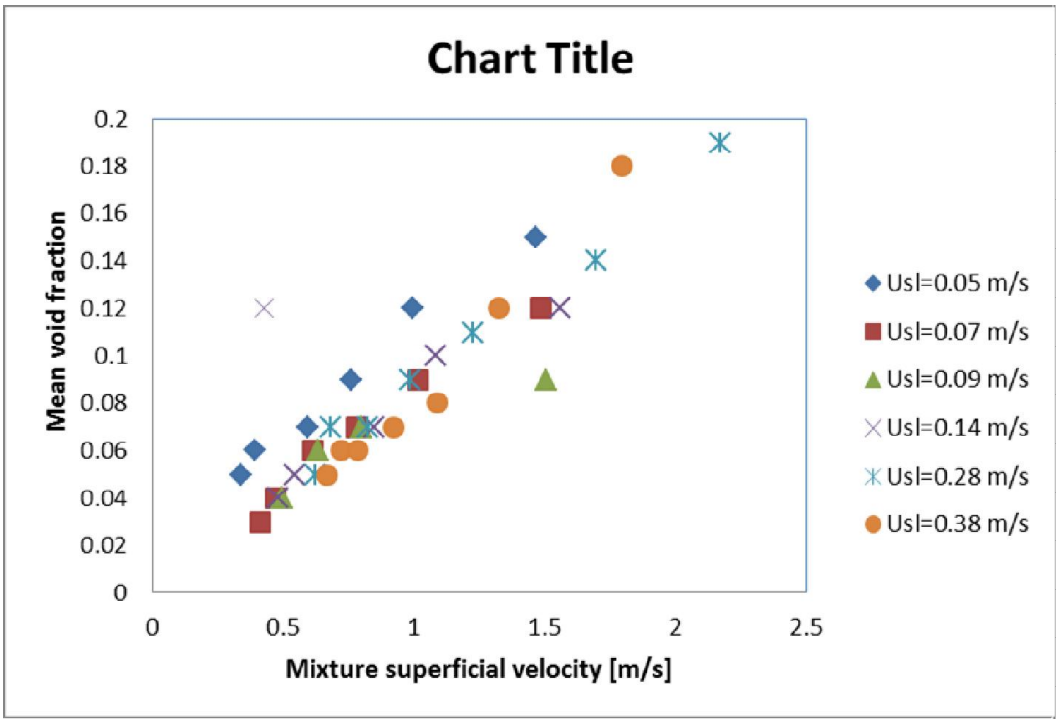

Figure 4.11: The determined mean void fraction in liquid slug at different liquid and mixture velocities

From figure 4.7 above it can be seen that the mean void fraction in liquid slug increases with increase in mixture superficial velocity .Moreover, the void in the slug body seems to be more influenced by the inlet gas velocities than the inlet silicone oil velocities. The slug voidage clearly increases with increasing mixture superficial velocity

4.6. Void fraction in Taylor bubble

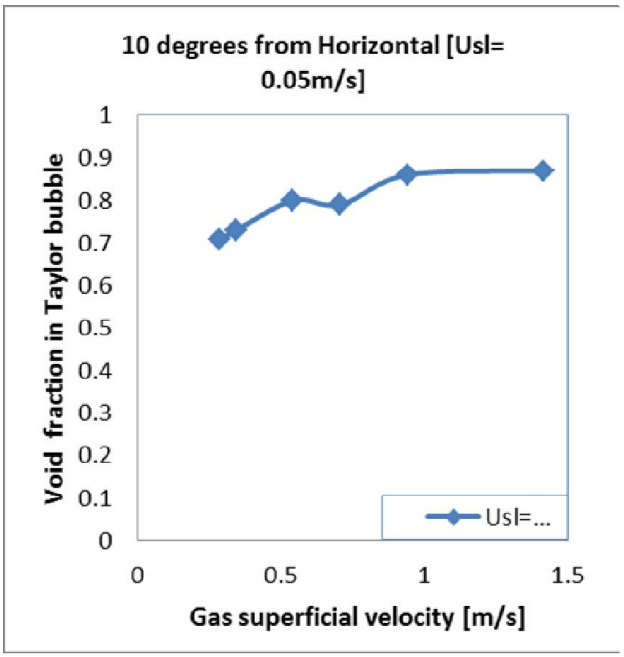

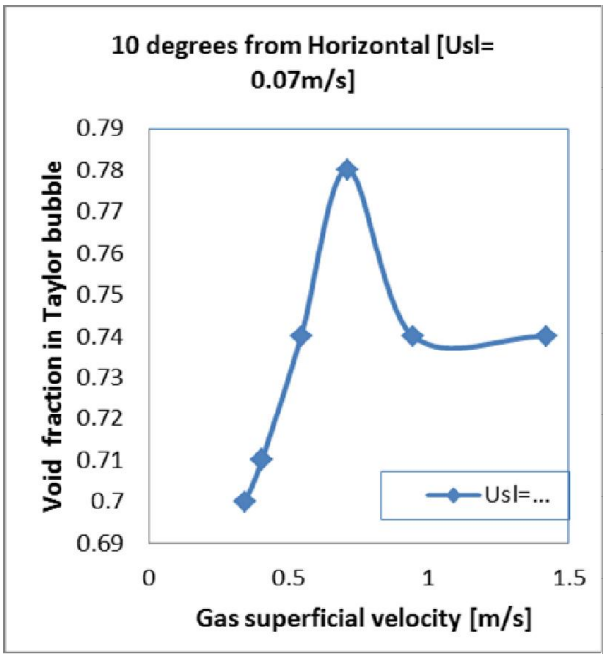

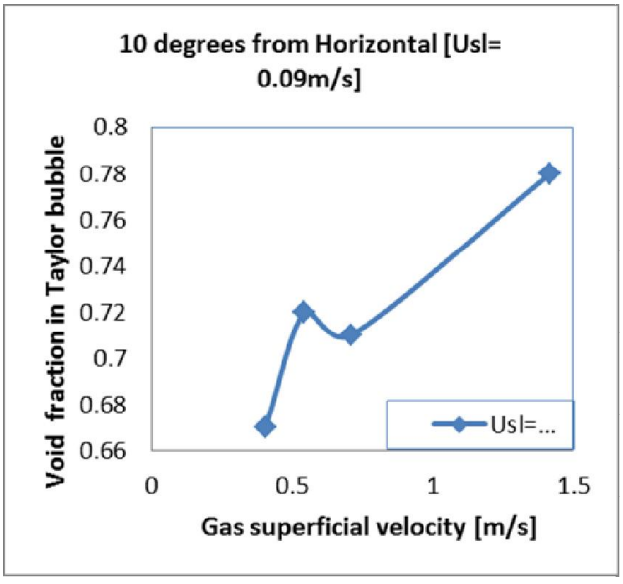

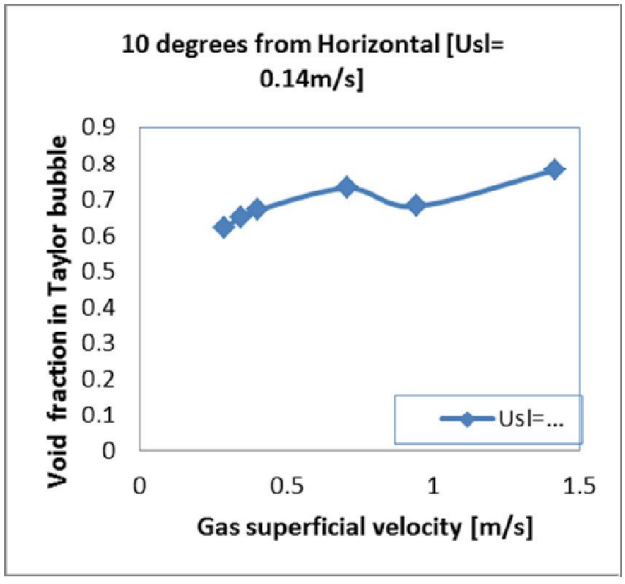

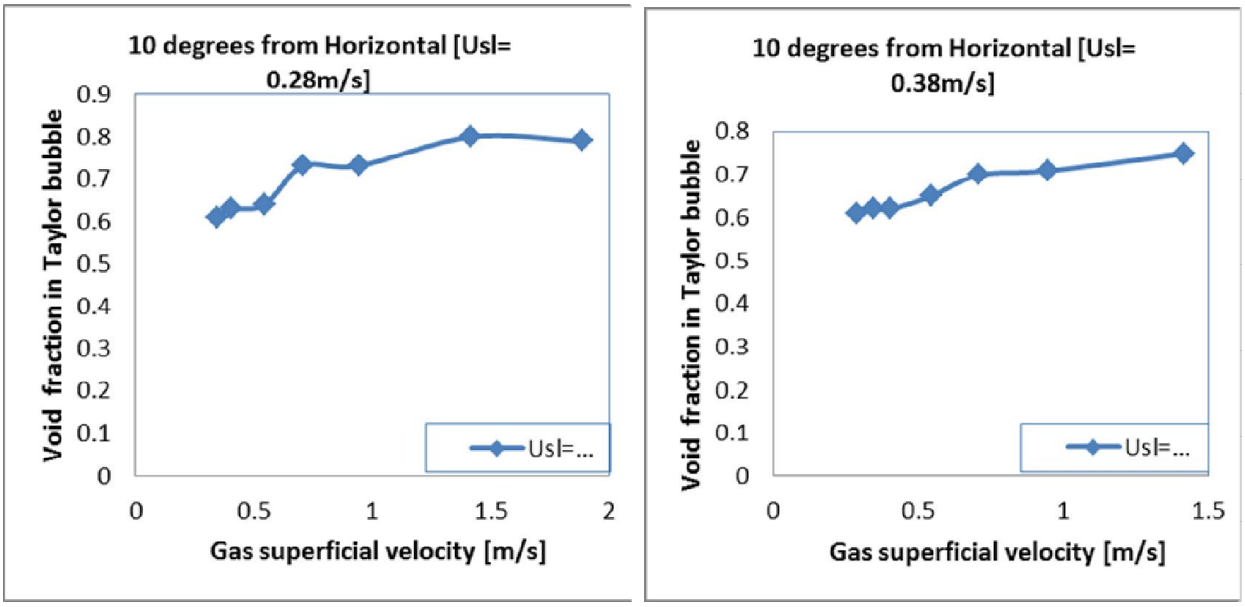

Figure 4.12: The determined void fraction in Taylor bubble at different liquid and gas superficial velocities

The gas void fraction, , is the volume of gas phase divided by the total volume of both gas and liquid phases. It is an important two-phase flow variable, as it may be used to define the occurrence of various flow regimes and is required for the prediction of, for example, the process pressure drop and the heat transfer coefficient; typically the hydrostatic pressure difference, which depends on the void fraction , is a significant term in the overall pressure drop. In practice, a number of factors, for example, the internal dimensions of the pipe work, the physical roperties of the gas, and liquid phases and flow rates (or superficial velocities), exert considerable influence and determine the flow regime.In an ideal void fraction against superficial gas velocity with constant liquid flow, there are three basic slope regimes: homogeneous, transition, and heterogeneous (Deckwer, 1992; Kastanek et al., 1993; Molerus, 1993; Zahradnik et al., 1997). These slope regimes are illustrated in Figure 4.8 using data obtained from a 0.067 m diameter bubble column using air–silicon oil data (Abdulkadir 2011). The homogeneous regime is

characterised by having a uniform dispersion of small spherical or ellipsoidal bubbles; it generally occurs at low gas superficial velocities. With increasing gas superficial velocity, void fraction in tailor bubble increases, and hence there is an increased probability of coalescence, leading to a broader bubble size distribution. Under some circumstances, coalescence leads to the transition regime, where is decreases in void fraction with increasing superficial gas velocity . At higher gas superficial velocities, the flow comprises large, irregularly shaped bubbles, which rise rapidly through a dispersion of smaller ellipsoidal bubbles (in air–water), and increases once more with increasing in the heterogeneous regime. Hills and Darton (1976) showed that the presence of small bubbles causes the large bubbles or gas slugs to rise much faster than they would do in isolation. In Figure 4.8, at liquid superficial velocity of 0.78 m/s, it can be seen clearly that the bubbles reach a maximum concentration at =0.4 and then start to coalesce; with increasing Usg , the transition from homogeneous to heterogeneous flow occurs, and falls.

4.7. Mixture density variation with gas superficial velocity

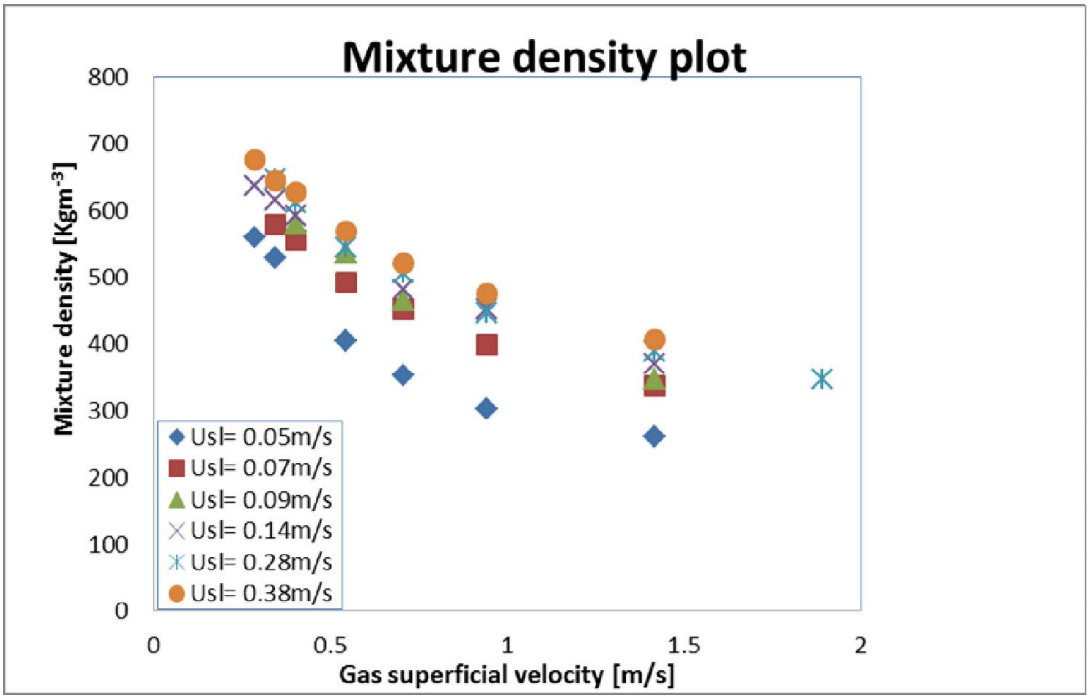

Figure 4.13: Influence of gas superficial velocity on mixture density at different liquid superficial velocities

Result from present studies presented in Figure 4.9 relates the influence of both gas and liquid superficial velocities to that of the mixture density. It was observed that as the gas superficial velocity increases, mixture density on the contrary decreases as expected. This may be attributed to the conversion of some of the liquid volume into Taylor bubbles as a result of high gas flow rate, i.e. the effect of entrainment of gas bubbles in the liquid slug, thereby increases the frictional pressure drop and reduces the liquid holdup. However, another interesting trend observed was that, as the liquid superficial velocity increases, the mixture density also increases. This may be attributed to some of the Taylor bubbles coalescing into liquid which increases the liquid volume, thereby, increases the liquid holdup and subsequently reduces the frictional pressure drop along the horizontal pipe.

4.8. Lengths of the liquid slug, Taylor bubble and the slug unit

4.8.1 Length of the liquid slug

The slug unit is divided in two regions, the liquid slug region, also called slug body, of length l_s and the liquid film region of length l_f. In order to calculate pressure drop in slug flow mechanistic models, it is necessary to know either the frequency or the slug length. Slug length will influence the size of downstream equipment used in a production facility. In fact some researchers such as Malnes (1983) think of the slug length as a more fundamental parameter than the frequency due to the fact that dimensionless slug length is expected to remain fairly constant for developed slug flow.

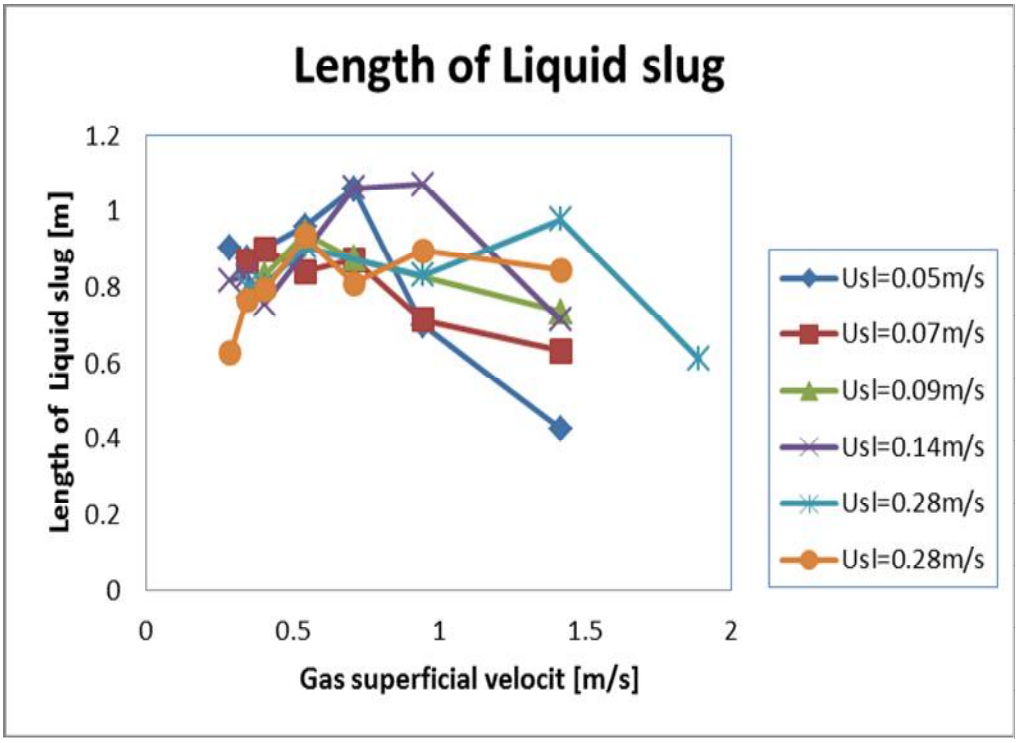

Figure 4.14: Variation of length of liquid slug with gas superficial velocity at different liquid superficial velocities

Figure 4.14 shows the mean length of tailor bubble l_{ls} versus the gas superficial velocity U_{SG} at different superficial liquid velocity U_{SL} along the pipe. The slug body length was estimated from the PDF plot of the different runs The resulting lengths of the liquid slug shows a similar trend as that observed by Dukler and Hubbard (1975) and Nichelson etal (1978) for the length of the liquid slug. The general trend between the variation of the length of liquid slug and the gas superficial velocity shows that an increase in the gas flow rate may increase bubble production, thereby bringing about an increase in the void fraction, which may lead to an increase in liquid slug length to a point and drops due to further increase in gas flow rate. also an increase in superficial liquid velocity initially leads to a decrease in length of tailor bubble to a point where it starts reducing again with further increase in liquid velocity. The increasing and decreasing alternating behavior observed in length of liquid slug could be attributed to an increase in bubble coalescence as a consequence of an increase in gas flow rate.

4.8.2 Length of Taylor bubble

Since intermittent flow is a stochastic phenomenon, the length of taylor bubble l_{tb} will be different for every slug moving along the pipe, being widely dispersed around its average. It is generally accepted, that the process of growth or decay of slugs depends on the process of shedding from the rear and the pick-up of liquid at the nose . The average lengths of Taylor bubble as a function of the gas superficial velocity at various liquid superficial velocities are shown in Figure 4.13. It can be concluded that there is a general trend between the variation of the lengths of Taylor and the gas superficial velocity. Increase in the gas flow rate may increase bubble production, thereby bringing about an increase in the void fraction, which may lead to an

increase in lengths of Taylor. Although from literature it is expected that the increasing liquid slug length gets to a point and drops due to further increase in gas flow rate, it is noticed that generally the liquid slug length here keeps increasing with increase in gas superficial velocity. Also as the liquid superficial velocity increases from 0.05 m/s to 0.38 m/s, the liquid slug length also drops with the highest drop noticed at higher gas superficial velocity. For a liquid superficial velocity of 0.05 m/s, the length of the liquid slug was observed to increase from 0.3994 m at a gas superficial velocity of 0.288 m/s to 4.2185 m at a superficial velocity of 1.418 m/s. At a liquid superficial velocity of 0.07 m/s, the length of the liquid slug was observed to increase from 0.3663 m at a gas superficial velocity of 0.344 m/s to 2.8958 m at a superficial velocity of 1.418 m/s.. At a liquid superficial velocity of 0.09 m/s, the length of the liquid slug increases sharply from 0.3543 m at a gas superficial velocity of 0.404 m/s to 2.7435 m at a superficial gas velocity of 1.418 m/s. At a liquid superficial velocity of 0.14 m/s, the length of the liquid slug gradually increased from 0.1736 m at a gas superficial velocity of 0.288 m/s to 2.384 m at a gas superficial velocity of 1.418 m/s. At a liquid superficial velocity of 0.28 m/s, the length of the liquid slug unit was observed to gradually increase from 0.2325 m at a gas superficial velocity of 0.344 m/s to 2.8833 m at a gas superficial velocity of 1.891 m/s. At a liquid superficial velocity of 0.38 m/s, a gradual upward trend was also observed, the length of the liquid slug was observed to gradually increase from 0.00875 m at a gas superficial velocity of 0.288 m/s to 2.0370 m at a gas superficial velocity of 1.418 m/s. It can be observed that the lengths of Taylor bubble becomes shorter with an increase in liquid superficial velocity. This is due to the fact that the frequency of the slugging increases with an increasing liquid superficial velocity. This trend conforms to results obtained by Dukler and Hubbard (1975) and Nicholson *et. al*. (1978).

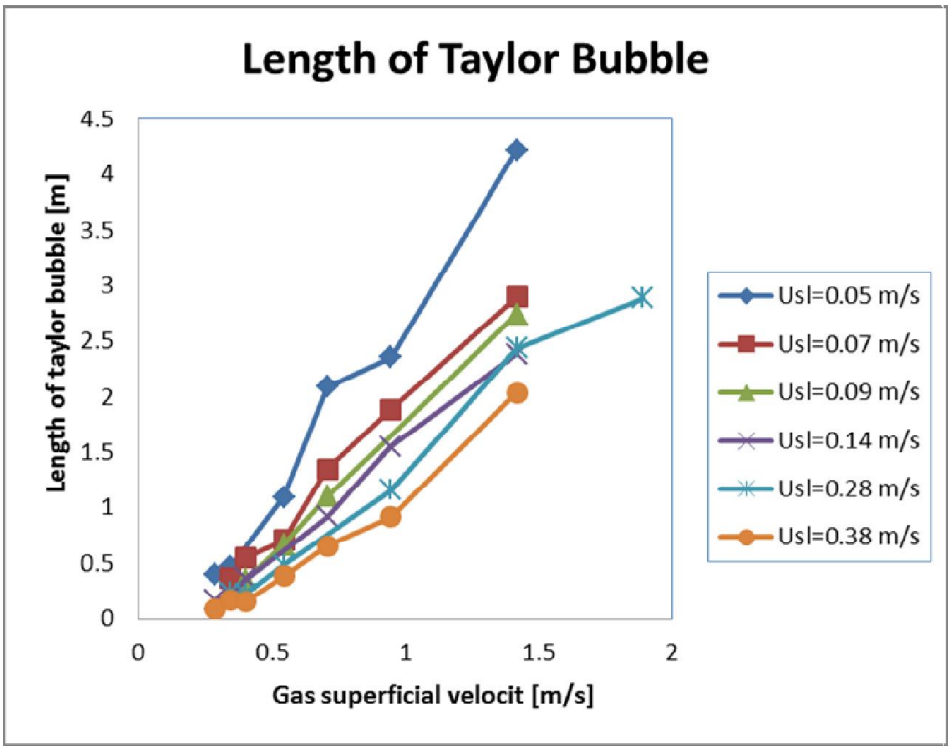

Figure 4.13 Variation of length of Taylor bubble with gas superficial velocity at different liquid superficial velocities

A similar observation was made by Nicholson *et. al.* (1978) and Banea and Brauner (1985). It was also observed that the length of the Taylor bubble is inversely proportional to the liquid film thickness

4.8.3 Length of liquid slug unit

The aggregated sum of the length of the liquid slug and the length of the Taylor bubble gives the length of the slug unit. The length of each slug unit was calculated from the measured velocities and slug frequencies. Figure 4.16 describes the variation of the length of slug unit with that of gas superficial velocity at different liquid superficial conditions.

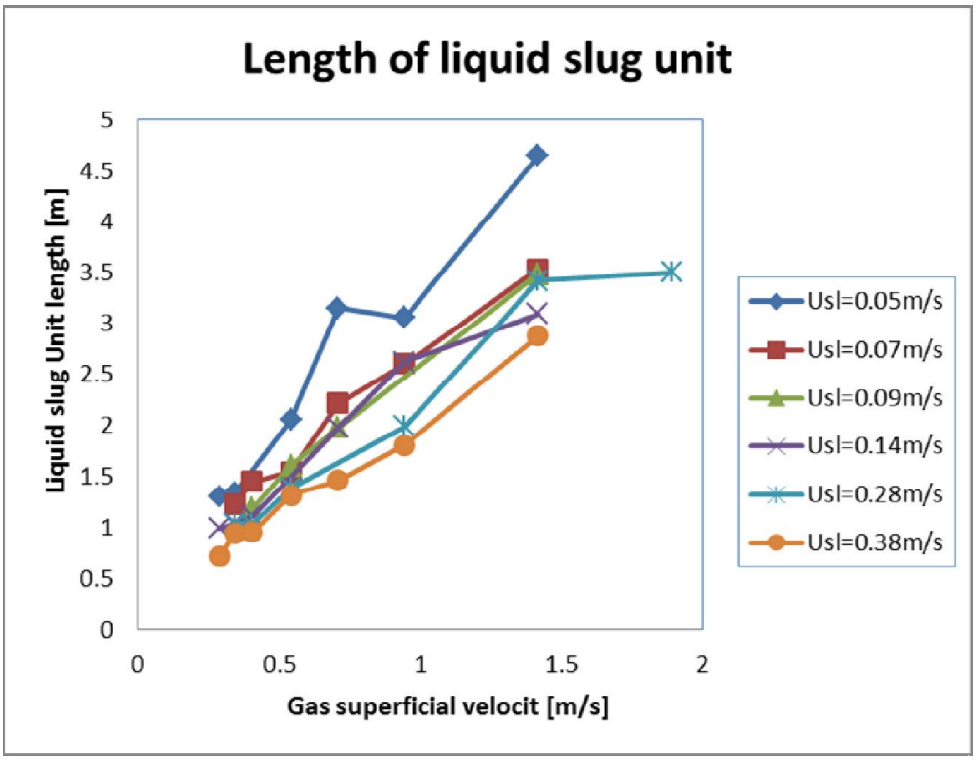

Figure 4.16: Variation of length of slug unit with gas superficial velocity at different liquid superficial velocities

The length of the slug unit on the other hand as opposed to the length of tailor bubble can be generally observed to increase with gas superficial velocity, which indicates a similar trend as the length of liquid slug.

However, it is worth noting that from the results presented in Figure 4.16, for increasing liquid superficial velocity, the slug unit length decreases and the short slugs units will be formed for sufficiently high liquid superficial velocities. This is an indication that the slug can grow by picking up liquid at the front from the stratified layer they move over. The front of a growing slug moves faster than its tail. As long as liquid is available at the slug front, the slug can grow. There is however a limit to the liquid level, indicated by a minimum holdup environment, below which the slug cannot take up any more liquid from the stratified layer. When the liquid in front of the slug drops to this level, the slug length cannot increase any longer; hence reach its maximum length. This pattern observed from the experimental result conforms to results obtained by Yamada *et. al*., (2008).

4.9 Slug frequency

Knowledge of slugging frequency is required as an input variable in many mechanistic models such as those of Dukler and Hubbard (1975) and Cook and Behnia (2000) and is relied upon for the design of separator vessels, Wren et al. (2005). In this work, the frequency was determined using an excel macro correlation and the results are plotted in Figures 5.10 and 5.11. It is in general affected by several parameters as described below.

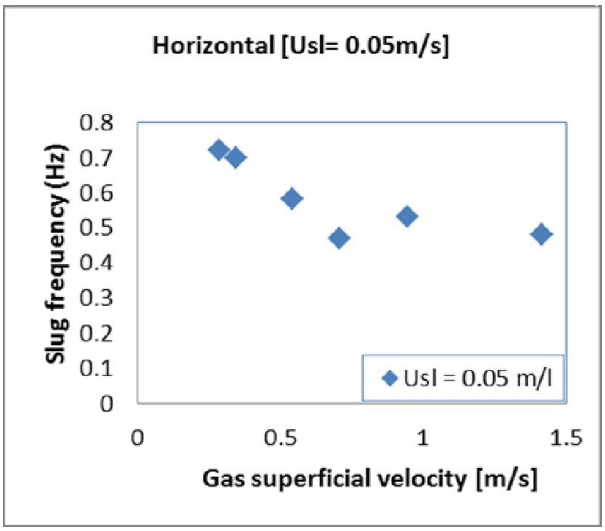
Horizontal [Usl= 0.05m/s]
Slug frequency (Hz)
0.8
0.7
0.6
0.5
0.4
0.3
0.2
0.1
0
0
0.5
1
1.5
Gas superficial velocity [m/s]
Usl = 0.05 m/l

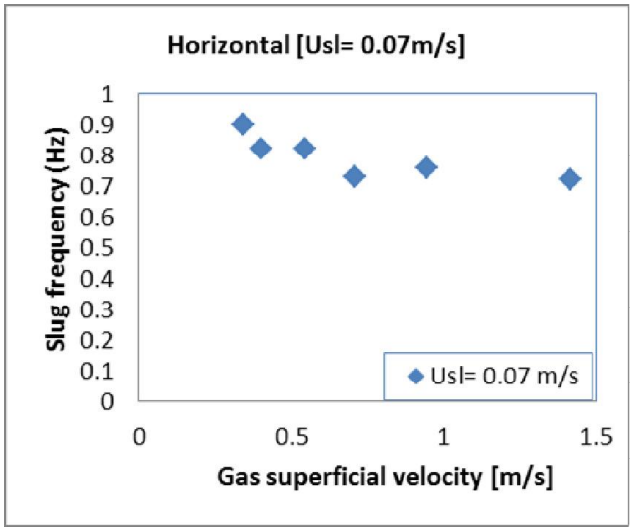
Horizontal [Usl= 0.07m/s]
Slug frequency (Hz)
1
0.9
0.8
0.7
0.6
0.5
0.4
0.3
0.2
0.1
0
0
0.5
1
1.5
Gas superficial velocity [m/s]
Usl= 0.07 m/s

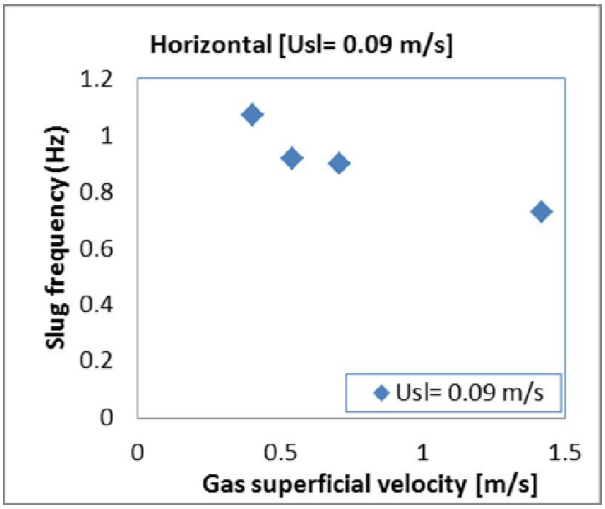
Horizontal [Usl= 0.09 m/s]
Slug frequency (Hz)
1.2
1
0.8
0.6
0.4
0.2
0
0
0.5
1
1.5
Gas superficial velocity [m/s]
Usl= 0.09 m/s

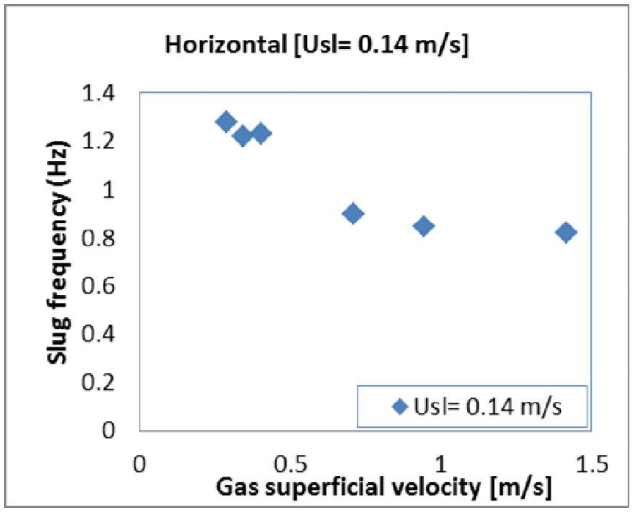
Horizontal [Usl= 0.14 m/s]
Slug frequency (Hz)
1.4
1.2
1
0.8
0.6
0.4
0.2
0
0
0.5
1
1.5
Gas superficial velocity [m/s]
Usl= 0.14 m/s

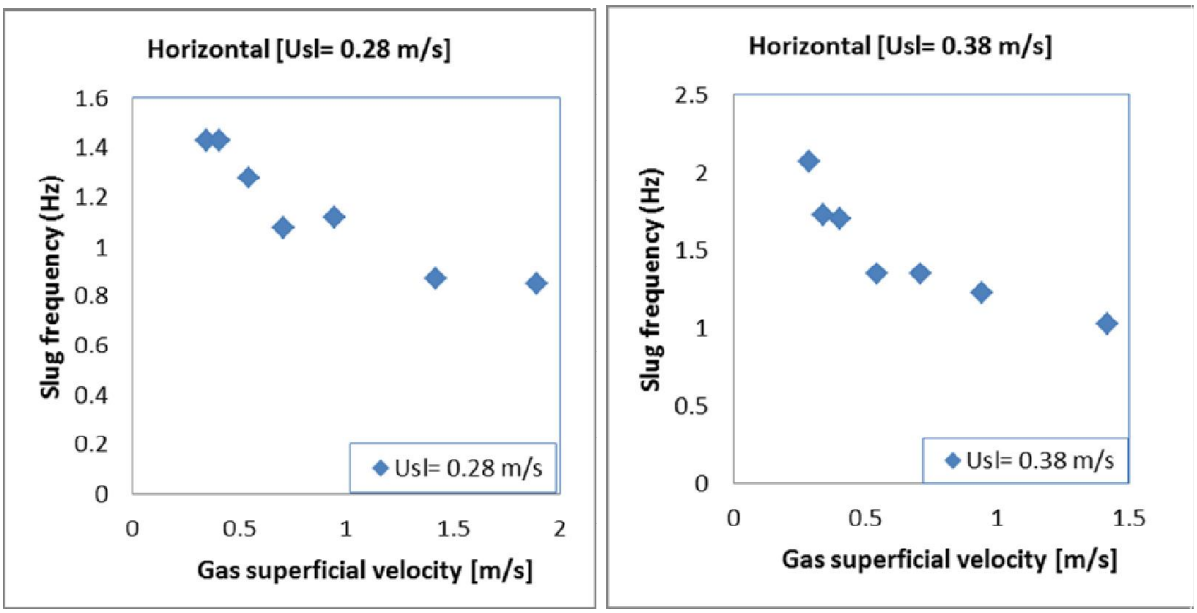

Figure 4.17: Variation of slug frequency with gas superficial velocity at different liquid superficial velocities

From the present studies, the slug frequency was calculated to lie between these range: 0.47 Hz ≤ Vs ≤ 2.07 Hz. In accordance with Abdulkadir etal (2014) the slug frequency of 10 degrees horizontal pipe behaves like its horizontal pipe counterpart It was observed that the slug frequency was found to generally decrease with increasing gas superficial velocity at lower liquid superficial velocities of 0.05 m/s, 0.07 m/s, 0.09 m/s and 0.14 m/s; hence the slug frequency intensity in this zone is low. However at higher gas superficial velocity of 0.28 m/s, an erratic behavior is observed. The slug frequency initially decreases from 1.43 Hz at 0.344 m/s to 1.08 Hz at 0.709 m/s and then increases to 1.12 Hz at 0.945 m/s and then subsequently decreases to 0.85 Hz with an increased superficial gas velocity of 1.891 m/s. However this erratic behavior was normalizes at higher liquid superficial velocity of 0.38m/s, the expected pattern was observed. The slug frequency increases with increasing gas superficial velocity. This behaviour can be attributed to the high liquid level in the pipe when the liquid superficial

velocity increases, which makes the slug frequency sensitive to changes in gas superficial velocities. At higher gas superficial velocities as stated in the literature, the gas phase suppresses liquid holdup. Therefore, it results in decreasing slug frequency. This observations support the findings of previous studies in horizontal gas-liquid flow including Taitel and Dukler (1977), Dukler and Hubbard (1975), and Jepson and Taylor (1993).

Experimental results were compared with the slug frequency correlation by Gregory and Scott (1969), Greskovich and Shrier (1972), Heywood and Richardson (1979), Nydal *et. al*. (1991) and Zabaras (1999) as shown in Figure 4.11.

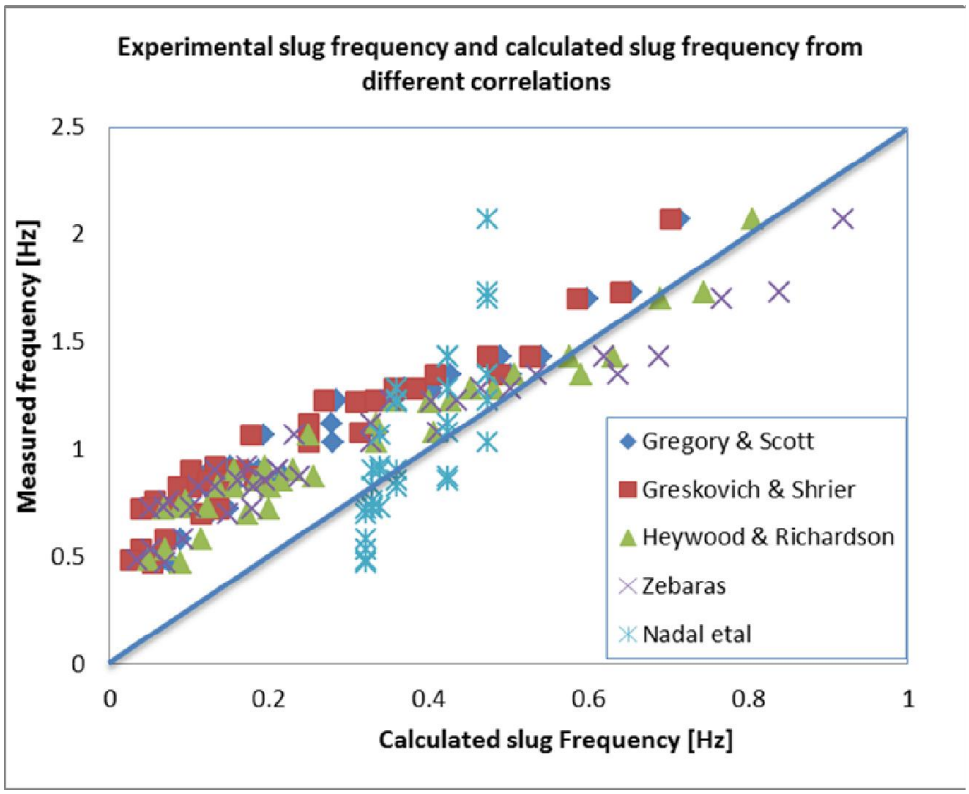

Figure 4.18: Comparison between experimental slug frequency and calculated slug frequency from different correlations

The literature review reveals that slug frequency data have been reported by several authors as well as correlations and a comprehensive comparison of correlations for slug frequency has been made in section 4.19, and a wide disagreement with the present data was found. Particularly for low superficial liquid velocity which is expected from the fact that none of the correlations for slug frequency found in the literature (except Zabaras (1999) for small inclination angles from the horizontal) take into consideration the effect of inclination angle. However, there is a better agreement between the present studies and the considered correlations at higher superficial velocity. Comparatively little has been reported on slug frequency data in inclined pipes, Van Hout et al. (2003) reported data on slug frequency for inclined flow but no model or correlation was proposed, their data exhibit a tendency similar to the one found in the present work (Figure 4.11) though their superficial velocities are lower.

Examination of the slug frequency compared with strictly horizontal pipes shows that slug frequency is strongly affected by the inclination angle as has been shown in Figure 4.11.its also worthy of mentioning that the correlations of Nadal etal gave the worst agreement to our experiment while Zebras gave the closest agreement due to its consideration of inclination in his correlation.

CHAPTER FIVE

CONCLUSION AND RECOMMENDATIONS

5.1 Conclusion

In this work, the experimental data obtained with a 67 mm diameter pipe have been presented. In these experiments the pipe was inclined to an angle of 10 degrees and the slug flow runs where characterized. In the first stage, visualisation of the flow patterns was carried out and flow patterns were identified on the flow pattern map. The scope of this work is to gain insight into gas-liquid intermittent slug flow. A full understanding of the hydrodynamics of slug flow in horizontal (0^o inclination) pipe makes the prediction of the slug flow characteristics much clearer. In this work, particular emphasis have been devoted to the investigation and understanding of the internal structure of air-silicone two-phase flow pattern in horizontal pipe using Electrical Capacitance Tomography (ECT) and to determine and have fundamental insight into the physical phenomena that govern the behavior of slug flow and the way these parameters behave under various conditions.

Some of the physical phenomena under the microscope of this work include: flow pattern map; slug frequency; void fraction in both Taylor bubble and liquid slug; film thickness, length of: the liquid slug, the Taylor bubble, the slug unit; translational (structure) velocity; etc.

The results obtained from present studies as described in the different results in chapter four, show interesting trends which confirm previous published works. For some of the parameters

determined, such as slug frequency, pressure drop, liquid holdup, translational (structure) velocity, they were compared with other empirical correlations to see how correlated they are.

- It has been shown that intermittent flow exists as the dominant flow pattern in upward inclined flow. The flow pattern obtained from the present studies depicts mostly smooth stratified and slug flow.

- For a constant liquid superficial velocity, the average liquid holdup decreases when the gas velocity is increased.
- When the result from the 10 degree upward pipe is compared with a horizontal pipe it is noticed that the pipe inclination has just a slight effect on the liquid holdup. The liquid holdup increased slightly for the higher inclination angles.
- when the result was compared with horizontal pipes Unlike the liquid hold up, the frequency is strongly affected by the inclination angle. At low gas superficial velocities, the frequency dependency on inclination is more appreciated
- In slug flow the expected linear dependence of the structure velocity on the mixture superficial velocity has been found. The experimentally measured translational velocity shows a The experimentally measured translational velocity shows a very good comparison with other published correlations used to determine translational velocity, although majority slightly under predicted due to the different assumptions made and experimental conditions under which their respective work took place.

- The liquid holdup in the liquid slug body appears to decrease with the gas superficial velocity
- Average slug lengths were in the order of 10 to 30 times the pipe diameter, and relatively independent of flow conditions. The slug length tends to decrease as the frequency increases and also with the inclination angle.
- The frequency is significantly affected by the change in the liquid flow rate. The slug frequency was found to generally decrease with increasing gas superficial velocity at lower liquid superficial velocity. However, at higher liquid superficial velocities, the slug frequency increases with increasing gas superficial velocity.
- The length: of slug, the Taylor bubble and slug unit, all show trends that conform with previous published studies.

5.2 Recommendations for further studies

Although this research work aims to carry out an extensive study on slug characterization in two-phase flow in 10 degrees inclined pipe using Electrical Conductance Tomography (ECT), there are still some issues that need further considerations.

- Further experiment on pressure drop should be carried out for 10 degree inclined pipes. Further investigation would confirm the effect of inclination to pressure drop
- More sophisticated instrumentation should be used (wire mesh sensor). This will allow obtaining the volume fraction distribution in the cross sectional area of the pipe and bubble size distribution.
- The use of a DP cell with a narrower range of pressure drop measurement for near horizontal inclinations; for these inclinations, the pressure drop is small and therefore this would allow more accurate measurements.
- Consideration should be paid to the use of other industrially relevant fluids like silicone oil, in order to investigate the effect of fluid properties (density, viscosity and surface tension), which would be of particular interest to the oil and gas industry applications.
- Since raw data was used to determine the physical phenomena, it is recommended that for subsequent studies, personal observation by the researcher would be key and relevant.
- Comparison should be made between experimental results obtained with that of computational fluid dynamics (CFD), to see the trend in fluid flow pattern with same fluid properties used in experimental work.
- Different pipe diameters, both bigger and smaller should be tested under this inclination in order to better characterise the effect of pipe diameter on the two -phase mixture parameters such as flow pattern and liquid holdup on 10 degrees inclined pipes.

NOMENCLATURE

A	Area, m^2
acc	Acceleration, ms^{-2}
ac	Alternate current, A
C	Constant= 2.48 x 10^-6
CO_2	Carbon dioxide
^oC	Degree Celsius
D	Drift
D, d	Diameter of pipe, mm, m
Dc	Direct current, A
DP	Differential Pressure
ECT	Electrical Capacitance Tomography
E_{OD}	Eotvos number for draft velocity $= \frac{\rho_L g d^2}{\sigma}$
f	Frequency, Hz
f	Liquid film
f_K	Flow friction factor
F_{rG}	Froude number $= \frac{U_m^2}{gd}$
fric	Frictional
FVC	Frequency to Voltage Converter
g	Acceleration due to gravity, $9.8ms^{-2}$
G	Gas
grav	Gravitational
H_f	Film holdup, Dimensionless
H_{fe}	Equilibrium film holdup, Dimensionless
H_{fw}	Wavy film holdup, Dimensionless

H_S	Liquid holdup in slug, Dimensionless
H_Z	Hertz
I.D	Internal diameter, mm
i	Indicate spatial coordinate
i	Indicates velocity component, number of a variable
j	Spatial coordinate
j_G	Gas superficial velocity, ms^{-1}
j_L	Liquid superficial velocity, ms^{-1}
L	Liquid
L_g	Length of gas (Tailor Bubble), m
LHS	Left Hand Side
LIF	Laser Induced Fluorescence
L_L	Length of liquid slug, m
L_s	Length of liquid slug, m
L_{su}	Length of the slug unit, m
L_{sui}	Individual length of slug unit, m
L_{TB}	Taylor bubble length, m
m	Mixture
m	meter
Max	Maximum
Min	Minimum
M_o	Morton's number, Dimensionless
N	Number
n	Number
N_f	Dimensionless inverse viscosity number, Dimensionless
PC	Personal computer
PDF	Probability Density Function

PIV	Particle Image Velocimetry
PSD	Power Spectral Density
PTL	Process Tomography Limited
PVC	Polyvinyl Chloride
R_e	Reynolds number $= \frac{\rho V D}{\mu}$, Dimensionless
R_{eL}	Slug Reynolds number, Dimensionless
RHS	Right Hand Side
s	Slug
SB-LOCA	Loss of Coolant Accident
t	Time, seconds
T	Absolute temperature, Kelvin
T or t	Translational, Turbulent
TSA	Time Series Analysis
$U_m = V_m$	Mixture superficial velocity , ms^{-1}
$U_S = V_S$	Slug velocity, ms^{-1}
$U_{SG} = V_{SG}$	Gas superficial velocity, ms^{-1}
$U_{SL} = V_{SL}$	Liquid superficial velocity, ms^{-1}
VBA	Visual Basic
V_{BF}	Gas bubble front velocity, ms^{-1}
V_D	Draft velocity, ms^{-1}
V_f	Film velocity, ms^{-1}
V_{fe}	Equilibrium film velocity, ms^{-1}
V_{fw}	Wavy film velocity, ms^{-1}
$V_G = G_G$	Velocity of gas, ms^{-1}
$V_L = G_L$	Velocity of liquid, ms^{-1}
Vs	Slug frequency, Hz
V_{SF}	Superficial film velocity, ms^{-1}

$V_T = V_t = V_{ST} = V_{TB}$	Translational velocity, Translational slug velocity, Structure velocity, ms^{-1}
X	Lockhart-Martinelli parameter, Dimensionless
$\left(\frac{dP}{dx}\right)_{fric.}$	Pressure drop due to frictional force, Nm^{-1}
$\left(\frac{dP}{dx}\right)_{grav.}$	Pressure drop due to gravity, Nm^{-1}
$\left(\frac{dP}{dx}\right)_{acc}$	Pressure drop due to acceleration, Nm^{-1}
$\left(\frac{dP}{dx}\right)_{K}$	Pressure gradient, Nm^{-1}

Greek Symbols

θ	Inclination angle
δ	Liquid film thickness, mm
θ_R	Pipe angle in radian
σ	Surface tension (Nm^{-1}); Stress tensor (Nm^{-1}); Standard deviation
σ_{water}	Surface tension of water, Nm^{-1}
ρ	Density, Kgm^{-3}
ρ_{air}	Density of air, Kgm^{-3}
ρ_{water}	Density of water, Kgm^{-3}
ρ_G	Gas density, Kgm^{-3}
ρ_L	Liquid density, Kgm^{-3}
μ	Viscosity, $Kgm^{-1}s^{-1}$
ω	Oscillating frequency, Hz
τ_i	Interfacial shear stress, Nm^{-1}
τ_w	Wall shear stress, Nm^{-1}
τ	Time displacement, seconds
λ	Wave length, Dimensionless gas phase parameter
ε, ε_g	Void fraction, Dimensionless
ε_{gs}	Void fraction in liquid slug, Dimensionless
ε_{TB}	Void fraction in the Taylor bubble, Dimensionless
μ	Viscosity, $Kgm^{-1}s^{-1}$
μ_{water}	Viscosity of water, $Kgm^{-1}s^{-1}$
μ_L	Liquid viscosity, $Kgm^{-1}s^{-1}$
μ_G	Gas viscosity, $Kgm^{-1}s^{-1}$
β	Pipe inclination, Radian
ϕ	Inclination angle, Radian
ψ	Dimensionless liquid phase parameter, Dimensionless

REFERENCES

Abdul-Majeed, G. H., (2000), "**Liquid slug holdup in horizontal and slightly inclined two-phase slug flow"**. *Journal of Petroleum Science and Engineering*, 27, pp. 29.

Abdulkadir, M., (2011), "**Experimental and Computational Fluid Dynamics (CFD) studies of gas-liquid flow in bends**" PhD thesis, University of Nottingham, UK.

Andreussi, P., Bendiksen, K. H. and Nydal, O. J., (1993), "**Void distribution in slug flow**". International Journal on Multiphase Flow, pp. 817.

Andritsos, N., Williams, L., and Hanratty, T. J., (1989), "**Effect of liquid viscosity on the stratified slug transition in horizontal pipe flow**". Int. 1. Multiphase Flow. Vol. 15. NO.6. pp. 877.

Arirachakaran, S., Oglesky, K.D., Malinowsky, M.S., Shoham, O., and Brill, P. (1989), "**An analysis of oil-water flow phenomenon in horizontal pipes**", SPE 18836, pp. 235.

Azzi, A., Azzopardi, B.J., Abdulkareem, L.A., Hilal, N., and Hunt, A., (2010), "**Study of fluidisation using electrical capacitance tomography**". 7th International Conference on Multiphase Flow, Tampa, Florida, USA May 30-June 4, pp. 1.

Azzopardi, B. J., Abdulkareem, L.A., Sharaf, S., Abdulkadir, M., Hernandez-Perez, V., and Ijioma, A., (2010), "**Using tomography to interrogate gas-liquid flow**". In: 28th UIT Heat Transfer Congress, Brescia, Italy, 21-23 June.

Bagci, S. and Al-Shareef, A. (2003), "**Characterisation of slug flow in horizontal and inclined pipes**". SPE 80930, pp.1

Baker, A., (1954), "**Simultaneous flow of oil and gas**", Oil and Gas J. Vol. 53. Pp.185

Baker, G., (2003), "**Separation and control of gas-liquid flows at horizontal T-junctions**". PhD thesis, University of Nottingham.

Baker, O., (1957), "**Discussion on how uphill and downhill flow affect pressure drop in two-phase pipelines in hilly country**", *Oil and Gas J.*, pp. 150-152.

Barnea, D. and Brauner, N., (1985), "**Holdup of liquid slug in two-phase intermittent flow**". Int.1. Multiphase Flow. Vol. 11, No.1, pp. 43.

Barnea, D., Shoham, O., Taitel, Y., (1980), "**Flow pattern characterization in two-phase flow by electrical conductance probe**". International Journal on Multiphase Flow 6: pp.394.

Beggs, H. D. and Brill, J. P., (1973), "**A study of two-phase flow in inclined pipes**". *J. Pet. Tech.,* pp. 607-617.

Bendat, J., and Piersol, A., (1980), "**Engineering application of correlation and spectral analysis**". John Wiley and Sons, New York, USA.

Bendiksen, K.H., (1984), "**An experimental investigation of the motion of long bubbles in inclined tubes**". International Journal Multiphase Flow 10, pp. 463.

Bendiksen, K.H. & Malnes, D., (1987), "**Experimental data on inlet and outlet effects on the transition from stratified to slug flow in horizontal tubes**". *Int. J. Multiphase Flow*, 13(1):131.135.

Benjamin, T.B., (1968), "**Gravity current and related phenomena**" Journal of Fluid Mechanics, Vol. 31, part 2, pp. 224.

Bolton, G.T., Korchinsky, W.J., and Waterfall, R.C., (1998), "**Calibration of capacitance tomography system for liquid-liquid dispersions**". Measurement Science Technology 9, pp.1977.

Bonnecaze, R. H., Erskine, W., and Grescovich, E. J., (1971), "**Holdup and pressure drop for two-phase slug flow in inclined pipelines**". *AIChE Journal*, Vol. 17, No. 5, pp. 1109-1113.

Brill, J. P., Schmidt, Z., Coberly. W. A., Herring, J. D., and Moore, D. W., (1981), "**Analysis of two-phase tests in large-diameter flow lines in Prudhoe Bay Field**". *SPE Journal, June 1981, pp.* 378.

Budi, S., Indarto, Deendarlianto, Thomas, S.W., (2012), **"Identification of gas-liquid co-current two-phase flow pattern in a horizontal pipe using the Power Spectral Density (PSD) and Artificial Neural Network (ANN)**". Modern Applied Science; Vol. 6, No. 9; pp.61-62

Butler, R. T., , X., and Bril, J. P., (1995), "**Ratio-Arm bridge capacitance transducer for two-phase flow measurements**". *ISA International Instrumentation Symposium*, Aurora, Colorado.

Cai, Y., Wambsganss, M.W., Jendrzejczyk, J.A., (1996), "**Application of chaos theory in identification of two-phase flow patterns and transitions in a small, horizontal, rectangular channel**". J Fluids Eng 118: pp387.

Coifman, R.R., Wickerhauser, M.V., (1992), "**Entropy-based algorithm for best basis selection**". IEEE Trans Information Theory 38: pp.716.

Carpintero-Rogero E., Kröss B., Sattelmayer T., (2006), "**Simultaneous HS-PIV and shadow graph measurements of gas-liquid flows in a horizontal pipe**" 13th Int. Symposium on Applications of Laser Techniques to Fluid Mechanics, (Lisbon), pp.26.

Carneiro J. N. E., Fonseca R. Jr., Ortega A. J., and Chucuya R. C., (2011) "**Statistical characterization of two-phase slug flow in a horizontal pipe**". XXXIII, pp. 253.

Cook, M.C., Newton, C.H., and Behma, M., (1995), "**Experimental investigation of air-water slug flow in horizontal pipes and comparism with existing models**". pp. 699.

Costigan, G., and Whalley, P. B., (1997), "**Slug flow regime identification from dynamic void fraction measurements in vertical air-water flows**". International Journal of Multiphase Flow 23, pp.276.

Czapp, M., Muller, C., Fernández, P. A., Sattelmayer, T., (2012), "**High-speed stereo and 2D PIV measurements of two-phase slug flow in a horizontal pipe**". 16th International Symposium on Applications of Laser Techniques to Fluid Mechanics Lisbon, Portugal.

Czapp M., Utschick M., Rutzmoser J., Sattelmayer T., (2012), "**Investigations on slug flow in a horizontal pipe using stereoscopic particle image velocimetry and CFD simulation with volume of fluid**". Proceedings of the 2012, 20th International Conference on Nuclear Engineering. Anaheim, USA.

Charles, M. E, Govier, G.W. and Hodgson, G.W., (1961), "**The horizontal pipeline flow of equal density oil-water mixture**". Can J.Chern. Eng. Pp.27.

Chen, J. J. J. and Spedding, P. L., (1981), "**An extension of the Lockhart-Martinelli theory of two-phase pressure drop**". *International Journal of Multiphase Flow* , Vol. 7, pp. 659-675.

Davies, R.M. and Taylor, G.I, (1950), "**The mechanics of large bubbles rising through extended liquid and through liquids in tubes**". *Proc. Roy. Soc. London,* 200A, pp.380.

de Chard, F. and Delhaye, J. M., (1996) "**A slug-churn flow model for small-diameter airlift pumps**". International Journal of Multiphase Flow 22, 627-628

Desai, J.B., Bambhamia, M.P., Siddala, S.S., Mehta, H.B. and Baneijee, J., (2011), "**Numerical simulation of Taylor slug flow in horizontal mini-channel**". 11th Asian International Conference on Fluid Mechanics and 3rd Fluid Power Technology Exhibition.

Dukler, A. E. & Hubbard, M. G., (1975), "**A model for gas-liquid slug flow in horizontal and near horizontal tubes**". Ind. Engng Chern. Fundam. 14, pp.345.

Fan, Z., Lusseyran, F., and Haniratty, T.J., (1993), "**Initiation of slugs in horizontal gas-liquid flows**". AICHE Journal, vol. 39, No.11; pp. 1741

Ferguson, M. E. G., and Spedding, P. L., (1995), "**Measurement and predication of pressure drop in two-phase flow**". *J. Chem. Tech. Biotechnol.*, 62, pp. 262.

Fernandes, R. C., Semiat, R., and Dukler, A.E., (1983), "**Hydrodynamics model for gas-liquid slug flow in vertical tubes**". *AIChE* Journal 29, pp.982.

Frank ,T.,(2005), " **Numerical simulation of slug flow regime for an air-water two-phase flow in horizontal pipes**". 11th International Topical Meeting on Nuclear Reactor Thermal-Hydraulics (NURETH-11), Avignon, France.

Fuchs, P. and Brandt, I. (1989), "**Liquid holdup in slugs. Some experimental results from the SINTEF two-phase flow laboratory**". paper presented at the 4th International Conference on Multi-Phase Flow, Nice,.

Gomez, L. E., Shoham, O. & Taitel, Y., (2000), "**Prediction of slug liquid holdup: horizontal to upward vertical flow**". *Int. J. Multiphase Flow*, 26, pp.522.

Govier, G.W., Radford, B.A., and Dunn, J.S.C., (1957), "**The upward vertical flow of air-water mixtures**". The Canadian Journal of Chemical Engineering 35, pp58.

Gregory, G. A. and Mattar, L., (1973), "**An In-situ volume fracture sensor for two-phase flows of non-electrolytes**". *The Journal of Canadian Petroleum Technology*, pp. 4.

Gregory, G.A. & Scott, D. S. (1969), "**Correlation of liquid slug velocity and frequency in horizontal concurrent as liquid flow**", pp.3.

Grescovich, E. J. and Shrier, A. L., (1971), "**Pressure drop and holdup in horizontal slug flow**". *AIChE Journal*, Vol. 17, No. 5, pp. 1214-1219.

Greskovich, E.J. and Shrier, A.L., (1972), "**Slug Frequency in Horizontal Gas-Liquid Slug Flow**". Ind. Eng. Chem. Proc. Design Dev., 11, pp.317.

Griffith, P. and Wallis, G. B., (1961), "**Two-phase slug flow**". *Trans. ASME Journal of Heat Transfer*, Vol. 83, pp. 307-320.

Hernandez-Perez, V., (2007), "**Gas-liquid two phase flow in inclined pipes**". PhD Thesis-University of Nottingham, School of Chemical, Environmental and Mining Engineering.

Hewitt G. F., (1978), "**Measurements of two-phase flow parameters**". London: Academic Press.

Heywood, N.I. and Richardson, J. F., (1979), "**Slug flow of air-water mixtures in a horizontal pipe: determination of liquid holdup by gamma-ray absorption**". *Chern. Eng.* Sci., 34, pp.17.

Holman, J.P., (2008), "**Experimental Methods for Engineers**". 8th edition, McGraw-Hill Inc, New York

Holt, A.J., (1996), "**Pressure drop and void fraction in narrow channels**". PhD thesis, University of Nottingham

Huang, S. M., Plaskowski, A.B., Xie, C.G., and Beck, M.S., (1989), "**Tomographic imaging of two-component flow using capacitance sensors**". Journal of Physics. E: Science and Instrumentation 22, pp. 176.

Huang, Z., Wang, B., and Li, H., (2003), "**Application of electrical capacitance tomography to the void fraction measurement of two-phase flow**". IEEE Transactions on Instrumentation and Measurement 52, pp.11.

Hubbard, M. G., (1965), "**An analysis of horizontal gas-liquid slug**". PhD Thesis, University of Houston.

Hubbard M.G., Duckler A.E., (1966), "**The characterisaton of flow regimes for horizontal two-phase flow**". Proceedings of the 1966 Heat Transfer Fluid Mechanics Institute. Stanford University Press, Stanford, pp. 119,

Jayanti, S., Hewitt, G.F. & White, S.P., (1990) "**Time-dependent behaviour of the liquid film in horizontal annular flow**". Int. Journal of Multiphase Flow. Vol. 16.

Jepson, W. P and Taylor, R .E., (1989), "**Slug flow and its transition in large diameter horizontal pipes**". Harwell Laboratory. AERE-RI29922

Jepson, W. P. and Taylor, R. E., (1993), "**Slug flow and its transitions in large-diameter horizontal pipes**". *International Journal of Multiphase Flow*, Vol. 19, No. 3, pp. 411-420.

Jones, O.C. Jr., Zuber, N. (1975), "**The interrelation between void fraction fluctuations and flow patterns in two-phase flow**". International Journal on Multiphase Flow 2: pp.288

Khatib, Z., and Richardson, J. F., (1984) "**Vertical co-current flow of air and shear thinning suspensions of kaolin**". Chemical Engineering Research and Design 62,139-154

Kouba, G. E., (1986), "**Dynamic calibration of two types of capacitance sensors used in measuring liquid holdup in two-phase**". *Proceedings of the 32nd ISA International*, Seattle.

Kouba, G. E., Shoham, O., and Brill, J. P., (1990), "**A nonintrusive flow metering method for two-phase intermittent flow in horizontal pipes**". *SPE Production Engineering*, Vol. pp. 378.

Kristiansen, O., (2004), "**Experiments on the transition from stratified to slug flow in multiphase pipe flow**". Ph.D. Thesis, NTNU, Trondheim, Norway.

Kouba, G. E., (1987), "**Horizontal slug flow modelling and metering**". PhD thesis, Dept. of Petroleum Engineering, University of Tulsa OK.

Laurinat, J. E., Hanratty, T. J., Jepson, W. P., (1985) "**Film thickness distribution for gas-liquid**
annular flow in a horizontal pipe". PhysicoChem. Hydrodynam. 6, 179-195.

Lin, P.Y. and Hanratty, T.J., (1986), "**Prediction of the initiation of slugs with linear stability theory**". *Int.* 1 *MultiphaseFlow, 12, pp.89*.

Lindken R., Merzkirch W., (2002), "**A novel PIV technique for measurements in multiphase flows and its application to two-phase bubbly flows**". Experiments in Fluids, 33; pp.819.

Lun, I., Calay, R. K., and Holdo, A. E., (1996), "**Modelling two-phase flows using CFD** ", *Applied Energy*, Vol. 53, No. 3, pp.301.

Marcano, R., , T. X., Sarica, C., and Brill, J. P., (1998), "**A Study of slug characteristics for two-phase horizontal flow**". SPE 39856*, pp.*214.

Mallat, S.G., (1989), "**Multi-resolution approximations and wavelet orthonormal bases of L2(R)**". Trans Am Math Soc 315: pp.76

Maley, L., (1997), "**A study of slug characteristics in large diameter horizontal multiphase pipelines**". M.Sc. Thesis, Ohio University.

Mandhane, J. M, Gregory, G.A., and Aziz, K., (l974), "**A Flow Pattern Map for Gas-Liquid Flow in Horizontal Pipes**". International Journal on Multiphase Flow. Vol. I, pp.583

Manolis, I. G., Mendes-Tatsis, M.A., and Hewitt, G. F., (1995), "**The effect of pressure on slug frequency on two-phase horizontal flow**". Proceedings of the 2nd International Conference on Multiphase flow, Kyoto, Japan, April 3-7.

Moissis, R., and Griffith, P., (1962), "**Entrance effects in two-phase slug flow**". ASME Journal of Heat Transfer, 366-370.

Mantripragada, V., (1997), "**A Study of the effect of inclination on flow regime transitions, slug flow characteristics, and corrosion rates at low pressures**". M.Sc., Thesis, Ohio University.

Matsui, G. (1984), "**Identification of flow regimes in vertical two-phase flow using differential pressure fluctuations**". International Journal on Multiphase Flow 10: pp. 713

Matsui, G. (1986), "**Automatic identification of flow regimes in vertical two-phase flow using differential pressure fluctuations**". Nucl Eng Des 95: pp. 226.

Nicholson, K.; Aziz, K. & Gregory, G. A., (1978), "**Intermittent two phase flow in horizontal pipes, predictive models**". Can. J. Chern. Engng 56, pp. 659.

Norris, S. E., (2000), "**A Parallel Navier-Stokes Solver for Natural Convection and Free Surface Flow**". Ph.D. Dissertation, University of Sydney, Department of Mechanical Engineering.

Nydal, O and Andreussi, P., (1991), "**Gas entrainment in a long liquid slug advancing in a near horizontal pipe**". International Journal of Multiphase Flow 17 (1991), No. 2, pp. 180.

Operating Manual of ECT Issue 1 (2009) "**Fundamentals of ECT**". Software version 659 Firmware version 2.2 p1_48FSR system hardware. DLL TFLR5000_2_27.

Paras, S.V. & Karabelas, A.J., (1991) "**Properties of the liquid layer in horizontal annular flow**". International Journal of Multiphase Flow. Vol. 17.

Pereyra, E and Torres, C., (2005), "**FLOPATN_Flow pattern prediction and plotting computer code**". Computer code vx. 1.0, University of Tulsa, Tulsa, Oklahoma.

Russell, T. W. F, Hodgson, G.W and Govier, G.W., (l959), "**Horizontal pipeline flow of mixture of oil and water**". Can.J. Chem. Eng. Pp. 9.

Scott, S. L., (1987), "**Modeling slug growth in pipelines**". PhD dissertation, University of Tulsa, OK.

Scott, S.L. and Kouba, G.E., (1990), "**Advances in Slug Flow Characterization for Horizontal and Slightly Inclined Pipelines**". paper SPE 20628 presented at the 1990 SPE Annual Technical Conference and Exhibition, New Orleans, Sept. 23-26.

Scott, S.L., Shoham, O., and Brill, J.P., (1989), "**Prediction of slug length in horizontal, large diameter pipes**". SPE Production Engineering, pp. 335.

Shannak, B.A., (2008), "**Frictional pressure drop of gas-liquid two-phase flow in pipes**". J.Elsevier No. 36; pp. 6-7.

Shoham, O., (2006), "**Mechanistic modeling of gas-liquid two phase flow in pipes**". pp.354.

Soldati, A., Paglianti, A., Giona, M., (1996), "**Identification of two phase flow regimes via diffusional analysis of experimental time series**". Exp. Fluids 21: pp. 157

Spedding, P.L., Woods, G.S., Raghunathan, R.S., Watterson, J.K., (1998), "**Vertical two-phase flow. Part I: Flow regimes**". Chem. Eng Res Des 76: pp. 614.

Sun, J.Y. and Jepson, W.P., (1992), "**Slug flow characteristics and their effect on corrosion rates in horizontal oil and gas pipelines**". SPE 24787, pp216.

Taitel, Y., (1990), "**Flow pattern transition in two-phase flow**". Proceedings of the 9th International Heat Transfer Conference, vol 1. Hemisphere, Washington, DC, pp. 248

Taitel, Y., (2000), "**Two-phase gas-liquid flow short course - Fundamentals of multiphase flow modelling**". Department of Fluid Mechanics and Heat Transfer, Tel Aviv University.

Taitel, Y. and Barnea, D. (1990), "**A Consistent Approach for Calculating Pressure Drop in Inclined Slug Flow**". Chem Eng. Sci. 45, No.5, pp. 1199.

Taitel, Y, and Dukler A.E., (1976), "**A model for predicting flow regime transitions in horizontal and near horizontal gas - liquid flow**". AICRE Journal. Vol. 22, NO.1, pp. 52.

Taitel, Y., and Dukler, A.E., (1977), "**A model for slug frequency during gas-liquid flow in horizontal and near horizontal pipes**". International Journal of Multiphase flow 3, pp.589.

Tsoukalas, L.H., Ishii, M., Mi, Y., (1997), "**A neurofuzzy methodology for impedance-based multiphase flow identification**". Eng Appl Artif Intel 10: pp. 545

Tutu, N.K., (1982), "**Pressure fluctuations and flow pattern recognition in vertical two-phase gas–liquid flows**". International Journal on Multiphase Flow 8: pp. 445.

Vince, M.A. and Lahey R.T. Jr., (1982), "**Development of an objective flow regime indicator**". Int. Journal, Multiphase Flow 8: pp. 126.

Wallis, G. B. and Dobson J.E., (1973), "**The onset of slugging in horizontal stratified air-water flow**". Int. J. Multiphase Flow. Vol. 1.pp. 173.

Wang, S.J., Dyakowski, T., Xie, C.G., Williams, R. A., and Beck, M.S., (1995), "**Real time capacitance imaging of bubble formation at the distributor of a fluidized bed**". Chemical Engineering Journal 56, pp. 102.

Weber, M.E., (1981), "**Drift in intermittent two-phase flow in horizontal pipes**". Cana. J .Chem. Eng. 59: 398-399.

Weisman, J. and King, J., (1981), "**Effect of fluid properties and pipe diameter on two-phase flow patterns in horizontal lines**". International Journal of Multiphase Flow, 5: pp. 462.

Woods, B.D. & Hanratty, T.J., (1999), "**Influence of the froude number on physical processes determining frequency of slugging in horizontal gas-liquid flows**". *Int. J. Multiphase Flow*, 25
(6-7):1195.1223.

Xiao, J. J., Shoham, O. and Brill J. P., (1990), "**A Comprehensive mechanistic model for two-phase flow in pipelines**". SPE paper 20631 presented at the SPE 65th Annual Technical Conference and Exhibition, New Orleans, LA.

Xie, C.G., Huang, S.M., Hoyle, B.S., Thorn, R., Lenn, C., Snowden, D., and Beck, M.S., (1992), "**Electrical capacitance tomography for flow imaging: system model for development of image reconstruction algorithms and design of primary sensors**". IEE Proceedings G 139, pp. 92.

Yamada, Y., Goto, Y., Endo, S., (2008), "**Characteristics of a flow distribution of gas-liquid slug flow in the long conduit**". Report of the Research Institute of Industrial Technology, Nihon University; No. 92, pp. 9.

Yang, W. Q., (1996), "**Calibration of capacitance tomography system: a new method for setting measurement range**". Measurement Science Technology 7, pp. 869.

Zheng, G. H., (1991), "**Two-Phase Slug Flow in Hilly Terrain Pipelines**". Ph.D. Dissertation, University of Tulsa.

Zheng, G. H. and Brill, J.P., Shoham, O., (1992), "**An Experimental Study of Two-Phase Slug Flow in Hilly Terrain Pipelines**". SPE 24788, presented in the SPE 67th Annual Technical Conference and Exhibition, Washington, DC.pp. 233

Zukoski, E. E., (1966), "**Influence of viscosity, surface tension, and inclination angle on motion of long bubbles in close tubes**". Journal, Fluid Mechanics 25 (4): pp. 821-823

APPENDIX

DATA MATRIX

Table A.1 Processed data for 76 mm 10 degrees inclined pipe.

RUN	Usl (m/ s)	Usg (m/ s)	Um	VF-ls	VF-tb	Ls/Ltb	ε_{AVG}	δ(liquid film)	Ls	Ltb	Lu	f	V
3	0.05	0.288	0.338	0.05	0.71	0.4408	0.3769	12.93361906	0.399423	0.906132	1.305556	0.72	0.94
4	0.05	0.344	0.394	0.06	0.73	0.5311	0.4119	11.99988895	0.465803	0.877054	1.342857	0.7	0.94
6	0.05	0.544	0.594	0.07	0.80	1.1376	0.5501	8.653476601	1.091898	0.959826	2.051724	0.58	1.19
7	0.05	0.709	0.759	0.09	0.79	1.9746	0.6072	7.39578195	2.090328	1.058608	3.148936	0.47	1.48
8	0.05	0.945	0.995	0.12	0.86	3.3725	0.6645	6.191848744	2.357552	0.699052	3.056604	0.53	1.62
9	0.05	1.418	1.468	0.15	0.87	9.871	0.7109	5.254513192	4.218473	0.42736	4.645833	0.48	2.23
17	0.07	0.344	0.414	0.03	0.70	0.4224	0.3561	13.50917148	0.366254	0.867079	1.233333	0.9	1.11
18	0.07	0.404	0.474	0.04	0.71	0.6099	0.3825	12.78139423	0.549785	0.901435	1.45122	0.82	1.19
19	0.07	0.544	0.614	0.06	0.74	0.8378	0.4534	10.94278053	0.706044	0.842736	1.54878	0.82	1.27
20	0.07	0.709	0.779	0.07	0.78	1.5422	0.4967	9.890222894	1.346242	0.872936	2.219178	0.73	1.62
21	0.07	0.945	1.015	0.09	0.74	2.6458	0.5563	8.513850337	1.89067	0.714593	2.605263	0.76	1.98
22	0.07	1.418	1.488	0.12	0.74	4.5825	0.6248	7.020162387	2.895843	0.631935	3.527778	0.72	2.54
31	0.09	0.404	0.494	0.04	0.67	0.4256	0.3544	13.55694607	0.354343	0.832573	1.186916	1.07	1.27
32	0.09	0.544	0.634	0.06	0.72	0.706	0.4026	12.24399261	0.665732	0.942963	1.608696	0.92	1.48
33	0.09	0.709	0.799	0.07	0.71	1.2571	0.4826	10.22774506	1.10153	0.876247	1.977778	0.9	1.78
35	0.09	1.418	1.508	0.09	0.78	3.728	0.615	7.228651538	2.743527	0.735925	3.479452	0.73	2.54
42	0.14	0.288	0.428	0.12	0.62	0.212	0.2934	15.35425256	0.173551	0.818637	0.992188	1.28	1.27
43	0.14	0.344	0.484	0.04	0.65	0.2545	0.316	14.66835111	0.211184	0.8298	1.040984	1.22	1.27
44	0.14	0.404	0.544	0.05	0.67	0.475	0.3422	13.90321583	0.358688	0.755133	1.113821	1.23	1.37
46	0.14	0.709	0.849	0.07	0.73	0.8624	0.4647	10.66341586	0.915827	1.061951	1.977778	0.9	1.78
47	0.14	0.945	1.085	0.1	0.68	1.45	0.4977	9.866468207	1.552701	1.070828	2.623529	0.85	2.23
48	0.14	1.418	1.558	0.12	0.78	3.3382	0.5896	7.776885881	2.383541	0.71402	3.097561	0.82	2.54
56	0.28	0.344	0.624	0.05	0.61	0.2898	0.2826	15.69135463	0.232542	0.802423	1.034965	1.43	1.48
57	0.28	0.404	0.684	0.07	0.63	0.2823	0.3212	14.5140394	0.227849	0.807116	1.034965	1.43	1.48
58	0.28	0.544	0.824	0.07	0.64	0.5338	0.3947	12.45357334	0.483972	0.906653	1.390625	1.28	1.78
59	0.28	0.709	0.989	0.09	0.73	0.8841	0.4379	11.33170564	0.065173	0.073716	0.138889	1.08	0.15
60	0.28	0.945	1.225	0.11	0.73	1.3932	0.5043	9.710282158	1.159101	0.83197	1.991071	1.12	2.23
61	0.28	1.418	1.698	0.14	0.80	2.4861	0.5673	8.268027723	2.434535	0.979259	3.413793	0.87	2.97
62	0.28	1.891	2.171	0.19	0.79	4.7204	0.6157	7.213704616	2.883301	0.610817	3.494118	0.85	2.97
68	0.38	0.288	0.668	0.05	0.61	0.1395	0.2492	16.77682147	0.087529	0.627447	0.714976	2.07	1.48
69	0.38	0.344	0.724	0.06	0.62	0.221	0.2837	15.65672886	0.169491	0.766926	0.936416	1.73	1.62
70	0.38	0.404	0.784	0.06	0.62	0.2016	0.3036	15.0415304	0.159881	0.79306	0.952941	1.7	1.62
71	0.38	0.544	0.924	0.07	0.65	0.4092	0.3676	13.18894144	0.382868	0.93565	1.318519	1.35	1.78
72	0.38	0.709	1.089	0.08	0.70	0.8103	0.4202	11.78435011	0.656488	0.810179	1.466667	1.35	1.98
73	0.38	0.945	1.325	0.12	0.71	1.0181	0.4718	10.48962082	0.914634	0.898374	1.813008	1.23	2.23
74	0.38	1.418	1.798	0.18	0.75	2.4063	0.5483	8.694160466	2.036977	0.846518	2.883495	1.03	2.97

Table A.2 Processed data for correlation between experimental translational (structure) velocity and other empirically determined structure velocity.

RUN	Usl (m/ s)	Usg (m/ s)	Um	Experimetal	Bendiskin	Weber	Benjamin
3	0.05	0.288	0.338	0.94	0.88599488	0.823064	0.84339
4	0.05	0.344	0.394	0.94	0.95319488	0.890264	0.91059
6	0.05	0.544	0.594	1.19	1.19319488	1.130264	1.15059
7	0.05	0.709	0.759	1.48	1.39119488	1.328264	1.34859
8	0.05	0.945	0.995	1.62	1.67439488	1.611464	1.63179
9	0.05	1.418	1.468	2.23	2.24199488	2.179064	2.19939
17	0.07	0.344	0.414	1.11	0.97719488	0.914264	0.93459
18	0.07	0.404	0.474	1.19	1.04919488	0.986264	1.00659
19	0.07	0.544	0.614	1.27	1.21719488	1.154264	1.17459
20	0.07	0.709	0.779	1.62	1.41519488	1.352264	1.37259
21	0.07	0.945	1.015	1.98	1.69839488	1.635464	1.65579
22	0.07	1.418	1.488	2.54	2.26599488	2.203064	2.22339
31	0.09	0.404	0.494	1.27	1.07319488	1.010264	1.03059
32	0.09	0.544	0.634	1.48	1.24119488	1.178264	1.19859
33	0.09	0.709	0.799	1.78	1.43919488	1.376264	1.39659
35	0.09	1.418	1.508	2.54	2.28999488	2.227064	2.24739
42	0.14	0.288	0.428	1.27	0.99399488	0.931064	0.95139
43	0.14	0.344	0.484	1.27	1.06119488	0.998264	1.01859
44	0.14	0.404	0.544	1.37	1.13319488	1.070264	1.09059
46	0.14	0.709	0.849	1.78	1.49919488	1.436264	1.45659
47	0.14	0.945	1.085	2.23	1.78239488	1.719464	1.73979
48	0.14	1.418	1.558	2.54	2.34999488	2.287064	2.30739
56	0.28	0.344	0.624	1.48	1.22919488	1.166264	1.18659
57	0.28	0.404	0.684	1.48	1.30119488	1.238264	1.25859
58	0.28	0.544	0.824	1.78	1.46919488	1.406264	1.42659
59	0.28	0.709	0.989	0.15	1.66719488	1.604264	1.62459
60	0.28	0.945	1.225	2.23	1.95039488	1.887464	1.90779
61	0.28	1.418	1.698	2.97	2.51799488	2.455064	2.47539
62	0.28	1.891	2.171	2.97	3.08559488	3.022664	3.04299
68	0.38	0.288	0.668	1.48	1.28199488	1.219064	1.23939
69	0.38	0.344	0.724	1.62	1.34919488	1.286264	1.30659
70	0.38	0.404	0.784	1.62	1.42119488	1.358264	1.37859
71	0.38	0.544	0.924	1.78	1.58919488	1.526264	1.54659
72	0.38	0.709	1.089	1.98	1.78719488	1.724264	1.74459
73	0.38	0.945	1.325	2.23	2.07039488	2.007464	2.02779
74	0.38	1.418	1.798	2.97	2.63799488	2.575064	2.59539

Table A.3 Processed data for correlation between experimental frequency and other empirically determined frequency.

RUN	Usl (m/ s)	Usg (m/ s)	Um	frequency	Gregory & Scott	Greskovich & Shrier	Heywood & Richardson	Zebaras	Nadal etal
3	0.05	0.288	0.338	0.72	0.147827176	0.136867458	0.200610069	0.17905843	0.321663852
4	0.05	0.344	0.394	0.7	0.126738445	0.114149906	0.171930046	0.149339157	0.321663852
6	0.05	0.544	0.594	0.58	0.088644379	0.070576206	0.114250239	0.092336504	0.321663852
7	0.05	0.709	0.759	0.47	0.075704252	0.053290367	0.089980615	0.069724051	0.321663852
8	0.05	0.945	0.995	0.53	0.068025673	0.039447921	0.069681592	0.051616886	0.321663852
9	0.05	1.418	1.468	0.48	0.067585161	0.02640789	0.049541735	0.034561261	0.321663852
17	0.07	0.344	0.414	0.9	0.174597644	0.161229973	0.230582567	0.210933384	0.330018409
18	0.07	0.404	0.474	0.82	0.152605585	0.137499002	0.201396617	0.179888619	0.330018409
19	0.07	0.544	0.614	0.82	0.120706615	0.101713253	0.155872129	0.13307446	0.330018409
20	0.07	0.709	0.779	0.73	0.100895659	0.077487751	0.123693151	0.101384023	0.330018409
21	0.07	0.945	1.015	0.76	0.087418869	0.057811225	0.096429053	0.075645492	0.330018409
22	0.07	1.418	1.488	0.72	0.081146302	0.039033324	0.069058598	0.051085262	0.330018409
31	0.09	0.404	0.494	1.07	0.19281486	0.17710784	0.249746651	0.231709369	0.338480077
32	0.09	0.544	0.634	0.92	0.152158929	0.1325225	0.195183784	0.173383956	0.338480077
33	0.09	0.709	0.799	0.9	0.12588673	0.101812232	0.15600105	0.133210677	0.338480077
35	0.09	1.418	1.508	0.73	0.094740993	0.052103435	0.088274234	0.068191574	0.338480077
42	0.14	0.288	0.428	1.28	0.369258772	0.356169667	0.452278504	0.465969498	0.36010285
43	0.14	0.344	0.484	1.22	0.323055315	0.308250778	0.400005635	0.403282288	0.36010285
44	0.14	0.404	0.544	1.23	0.285470303	0.268906108	0.356170645	0.351812227	0.36010285
46	0.14	0.709	0.849	0.9	0.186458119	0.161631019	0.231069998	0.211480621	0.36010285
47	0.14	0.945	1.085	0.85	0.154497241	0.123638515	0.184004426	0.161784268	0.36010285
48	0.14	1.418	1.558	0.82	0.128579143	0.085848718	0.134949506	0.112359285	0.36010285
56	0.28	0.344	0.624	1.43	0.54130462	0.526925819	0.630934991	0.68939432	0.424208012
57	0.28	0.404	0.684	1.43	0.490028688	0.47415894	0.576810169	0.62036715	0.424208012
58	0.28	0.544	0.824	1.28	0.403106233	0.383950143	0.482093376	0.502362554	0.424208012
59	0.28	0.709	0.989	1.08	0.336640628	0.313836641	0.406158603	0.410648621	0.424208012
60	0.28	0.945	1.225	1.12	0.277878604	0.250097426	0.334880913	0.327277944	0.424208012
61	0.28	1.418	1.698	0.87	0.219649109	0.182262628	0.255911934	0.238563511	0.424208012
62	0.28	1.891	2.171	0.85	0.195843204	0.148949448	0.215566177	0.195010951	0.424208012
68	0.38	0.288	0.668	2.07	0.713646839	0.702836175	0.805978667	0.91955378	0.473210705
69	0.38	0.344	0.724	1.73	0.653042808	0.641062947	0.745354934	0.83874559	0.473210705
70	0.38	0.404	0.784	1.7	0.598938388	0.585761445	0.690335523	0.76640423	0.473210705
71	0.38	0.544	0.924	1.35	0.503511956	0.487705647	0.59078801	0.638137832	0.473210705
72	0.38	0.709	1.089	1.35	0.426874395	0.408167588	0.507820576	0.534098925	0.473210705
73	0.38	0.945	1.325	1.23	0.35572408	0.333089847	0.42724279	0.435901238	0.473210705
74	0.38	1.418	1.798	1.03	0.280162704	0.250029443	0.334803537	0.327280904	0.473210705